Q. J. R. Meteorol. Soc. (2002), **128**, pp. 2663–2690 doi: 10.1256/qj.01.202

Entrainment in stratocumulus-topped mixed layers

By BJORN STEVENS*
University of California Los Angeles, USA

(Received 11 December 2001; revised 9 May 2002)

SUMMARY

Mixed-layer theory is used to synthesize and evaluate recently proposed entrainment parametrizations (rules) for the stratocumulus-topped boundary layer. The results illustrate that recently proposed entrainment rules exhibit marked differences. Significant differences are found between rules derived from a single set of simulations and rules derived from different sets of simulations. Such differences imply steady-state boundary layers that can differ by as much as a factor of two in climatologically important properties such as vertically integrated liquid water and boundary-layer depth. In addition, surface fluxes depend significantly on entrainment, as do different measures for the limits of applicability of the mixed-layer theory. Moreover, differences among proposed entrainment rules yield steady states with different equilibrium sensitivities; models closed with some rules are more sensitive to divergence while others are more sensitive to variations in the sea surface temperature. Overall we expect that these differences should be evident in the climatology and climate sensitivity of stratocumulus derived from models which use these rules. This degree of sensitivity encourages attempts to bound entrainment rules observationally, by requiring consistency with the observed stratocumulus climatology. The analysis also encourages the use of somewhat simpler strategies for the parametrization of the stratocumulus-topped boundary layer in large-scale models.

KEYWORDS: Boundary layers Clouds Mixing

1. INTRODUCTION

The marine stratocumulus-topped boundary layer (STBL), as often observed on the eastern ends of the summertime subtropical high-pressure zones, invites description and explanation. The early descriptive studies (cf. von Ficker 1936; Neiburger *et al.* 1961), which demonstrated the pervasiveness of this cloud regime, have been supported by modern satellite studies (e.g. Hartmann and Short 1980) which highlight the importance of this cloud regime to the Earth's radiative budget. Such studies have helped motivate theoretical analyses, in nearly all of which the mixed-layer framework of Lilly (1968) plays an essential role.

While on a fundamental level our understanding of the relationship between cloudiness and the large-scale environment has not increased markedly since 1968, there has been a steady percolation of new ideas regarding ways in which clouds, and in particular stratocumulus clouds, may affect climate. For instance, the question of how the atmospheric aerosol regulates cloudiness and hence climate has garnered much attention (e.g. Twomey 1974; Twomey 1977; Albrecht 1991; Pincus and Baker 1994, and others). Alternatively a number of other studies have focused on the role stratocumulus clouds play in larger-scale processes centred in the tropical eastern Pacific (e.g. Ma *et al.* 1996; Philander *et al.* 1996). For all of these questions our inability to realistically simulate the STBL in large-scale models has frustrated attempts to better understand our planet's climate. How can it be that what has generally been viewed as a successful and rather simple theory of the STBL, as proposed by Lilly over 30 years ago, has borne so little fruit?

Perhaps the chief reason is that the theory is based on an explicit equation for the top of the boundary layer which is difficult to implement within the context of most large-scale models—and so is rarely implemented. But even general-circulation models which have gone so far as to change their vertical coordinate to more elegantly incorporate

* Corresponding address: Department of Atmospheric Sciences, University of California Los Angeles, 405 Hilgard Ave., Box 951565, Los Angeles, CA 90095-1565, USA. e-mail: bstevens@atmos.ucla.edu

the mixed-layer theory of Lilly (i.e. Suarez *et al.* 1983) have struggled to realistically represent the STBL. In these cases it is generally thought that two assumptions in the mixed-layer theory may form a weak link. The first being an assumption about the domain of validity of the theory. The second being a specific hypothesis as to the rate at which boundary-layer turbulence mixes in air from the free troposphere, the so-called entrainment rate. These assumptions continue to be the subject of much inquiry.

For his first assumption Lilly postulated that cloudy steady states were only possible in regimes where the equivalent potential temperature increased across the top of the cloud layer. The idea being that if the equivalent potential temperature decreased across cloud top, mixtures of cloudy air and free-tropospheric air could become negatively buoyant. This was suggested as the basis for an instability which would increase the mixing between the cloud and its environment and rapidly evaporate the cloud. This idea (first proposed in this context by Kraus (1963), and amended by Randall (1980) and Deardorff (1980) to account for the effect of liquid water on buoyancy) has come to be known as cloud-top entrainment instability—CTEI. To account for observations which suggest that it is not relevant (e.g. Kuo and Schubert 1988) further modifications to the original idea have been suggested (e.g. MacVean and Mason 1990; Shy and Breidenthal 1990; Duynkerke 1993), most of which make different assumptions about the nature of the mixing processes. One reason that investigators insist on such a process is that attempts to use the mixed-layer theory in the absence of this constraint fail to predict the observed transition from stratocumulus to cumulus clouds, predicting instead stratocumulus over much of the world's oceans (Randall *et al.* 1985).

CTEI is, however, not the only means for limiting stratocumulus cloud incidence. Alternative hypotheses have recently been suggested which seem at least as compelling. For instance, Bretherton and Wyant (1997) suggested that the observed transition from a well mixed STBL to a more trade-cumulus-like regime is not at all due to CTEI. Instead, they posited that when surface fluxes become sufficiently important to the turbulent dynamics of radiatively forced stratocumulus layers it becomes energetically unfavourable to mix warm inversion air down to the surface, and instead a cumulus cloud layer forms. Stevens (2000) sharpened this criterion and demonstrated that indeed a cloud transition is readily evident in idealized fine-scale three-dimensional simulations of the STBL—thus lending further credence to the Bretherton and Wyant (1997) mechanism for the cloud transition. In addition, and perhaps somewhat less specifically investigated, is the role that drizzle may play in limiting the domain of mixed-layer theory. Observations (Paluch and Lenschow 1991) and simulations (Stevens *et al.* 1998) suggest that as clouds deepen drizzle limits their development and promotes the formation of a conditionally unstable cloud layer which favours cumulus convection. Thus, drizzle may also play a critical role in observed transitions between cloud regimes.

Lilly's second assumption, which we mostly focus on here, amounted to a hypothesis regarding the efficiency with which the STBL entrains air from the free troposphere. It has always been controversial. In the years following the introduction of the mixed-layer theory a number of alternative hypotheses were proposed, although little consensus emerged as to which ideas were correct. Interest in these questions was rekindled recently, when a comparison of large-eddy simulations (LESs) of the STBL (Moeng *et al.* 1996) illustrated that various simulations differed sharply in their prediction of the entrainment rate—with profound consequences for the evolution of the cloud layer. These results refocused attention on entrainment, spawning a number of subsequent studies (Lewellen and Lewellen 1998; Lock 1998; Bretherton *et al.* 1999; Moeng *et al.* 1999; Stevens *et al.* 1999; van Zanten *et al.* 1999) which have led to a new generation of entrainment rules—some of which are being implemented in larger-scale models.

However, it remains unclear how reliable the LES results are, the extent to which rules proposed by different groups resemble one another, and the extent to which differences that may exist might lead to systematic differences in predictions of cloudiness by the mixed-layer theory.

The need to critically evaluate the recent round of entrainment rules is further motivated by the realization that CTEI, the Bretherton and Wyant (1997) mechanism, and the propensity of clouds to deepen sufficiently to promote drizzle, are all potentially quite sensitive to what entrainment rule one uses. This connection between Lilly's first and second assumption has been noted in the past (e.g. Bretherton and Wyant 1997), but has not been significantly explored. For instance, could what seem like small differences in entrainment rules lead to large differences in regime boundaries as diagnosed by either CTEI or the Bretherton and Wyant (1997) mechanism? Another reason for investigating differences and similarities among entrainment rules, and their dynamical implications, is to help refine theoretical expectations for ongoing work (e.g. Lock 2000) with large-scale models. For instance, if one studies the sensitivity of the general circulation to varied entrainment rules, what might one expect to happen?

For all of the above reasons it seems worthwhile to study how recent work on closing the mixed-layer theory impacts on its behaviour. We do so by reviewing and unifying the various entrainment rules which have been proposed in the literature: essentially we focus on two questions: (1) how well do we really understand entrainment and (2) does it really matter? We answer the first question by exploring the relation between recently proposed entrainment rules, taking their uniformity as a measure of concord among various groups and methods. We answer the second by studying how the behaviour of a mixed-layer model depends on its entrainment closure. We also examine how various proposals for limiting the mixed-layer theory are affected by one's choice of rule.

2. Mixed-layer framework

The basic idea of applying mixed-layer theory to model the stratocumulus-topped boundary layer is motivated by the conceptual framework illustrated by the cartoon and data in Fig. 1. Here, a shallow, thermodynamically distinct, and relatively well mixed layer of air underlies the free troposphere. At its top is a cloud layer with cloud base being about where one would predict by adiabatically lifting parcels of air from the near-surface region. The cloud layer is capped by a temperature inversion which shows up as a region of sharply increasing potential temperature and sharply decreasing humidity. The data motivates the identification of three distinct layers: an outer layer ($z > z_{i+}$) where turbulent fluxes vanish, a mixed layer ($z < z_{i-}$), and an undulation layer ($z_{i+} > z > z_{i-}$) which subsumes the variations in cloud-top height. The undulation layer is often called an interfacial layer under the pretext that variations in cloud-top height are negligible.

If we know the state of the free troposphere, the structure of the mixed layer, and assume local thermodynamic equilibrium, the thermodynamic state of the system can be determined by two independent variables: one which describes the heat content of the lower layer, the other which describes its composition in terms of water mass. We work in terms of the layer-averaged values of the liquid-water static energy, $s_l = c_p T + gz - Lq_l$, and the total-water specific humidity, q_t, where all symbols retain their traditional meanings (i.e. C_p, T, L and q_l are the isobaric specific heat, temperature, latent heat of vaporization and liquid-water specific humidity, respectively). For the most

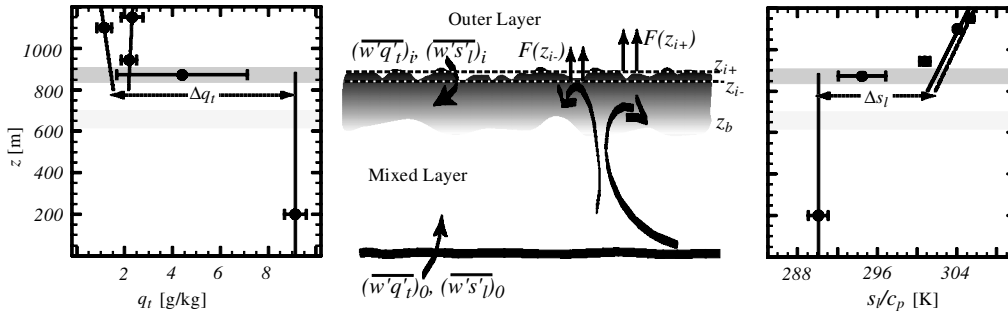

Figure 1. Schematic of stratocumulus-topped mixed layer, illustrating the structure of cloud top and cloud base (denoted z_b) and the levels where the radiation fluxes (denoted by F) and entrainment fluxes of liquid-water static energy ($\overline{w's'_l}$) and total-water specific humidity ($\overline{w'q'_t}$) are located. In the left and right panels respectively, we illustrate measured profiles of specific humidity and liquid-water static energy as derived from flight 5 of the first DYCOMS (Dynamics and Chemistry of Marine Stratocumulus) experiment. The temperature and moisture profiles in the outer layer are derived from regressions of two independent aircraft soundings of the free troposphere. The mixed-layer state and variability are determined by flight legs in the mixed layer (at the indicated height) and soundings. The variability in the undulation layer $z_{i-} \leqslant z \leqslant z_{i+}$ is determined by successive ascents and descents through cloud top, and the state just above z_{i+} is determined by a flight leg at this level. The variability of cloud base is estimated from soundings and the lifting condensation level of air near the surface.

part we work in terms of bulk values which we denote by angle brackets, e.g.

$$\langle s_l \rangle = \frac{1}{h} \int_0^h s_l(z, t)\, \mathrm{d}z. \tag{1}$$

Here, the x and y dependence in the integrand is suppressed by restricting ourselves to a consideration of horizontally homogeneous states, and $h = z_{i-}$ denotes the top of the mixed layer. Both s_l and q_t are effectively conserved for adiabatic transformations of the moist system, which means that for a layer that is well mixed, local values of s_l or q_t should not differ substantially from vertically averaged values. Although s_l is nonlinear, due to the dependence of c_p on the composition of the air (and hence q_t), we use a linearized variant in which variations of c_p with q_t are neglected. Because one of the most daunting aspects of moist thermodynamics is the notation, we include a list of recurrent symbols and a discussion of our notation in the appendix.

Thus, the evolution of the mixed-layer state is governed by equations for $\langle s_l \rangle$ and $\langle q_t \rangle$ respectively:

$$h\frac{\mathrm{d}}{\mathrm{d}t}\langle s_l \rangle = C_D \|\mathbf{U}\|(s_{l,s} - \langle s_l \rangle) + \left(\frac{\mathrm{d}h}{\mathrm{d}t} + Dh\right)\{s_l(z_+) - \langle s_l \rangle\} - \{\mathcal{F}_s(z_+) - \mathcal{F}_{s,0}\}, \tag{2}$$

$$h\frac{\mathrm{d}}{\mathrm{d}t}\langle q_t \rangle = C_D \|\mathbf{U}\|(q_{t,s} - \langle q_t \rangle) + \left(\frac{\mathrm{d}h}{\mathrm{d}t} + Dh\right)\{q_t(z_+) - \langle q_t \rangle\} - \{\mathcal{F}_q(z_+) - \mathcal{F}_{q,0}\}. \tag{3}$$

To derive these equations we have made a number of assumptions, all of which are typical. First we have assumed that the surface flux of s_l or q_t can be expressed using bulk-aerodynamic theory, where the exchange coefficient C_D is a weakly varying function of the local conditions, and $\mathbf{U}$ is the vector wind; second we have assumed that the divergence, D, of the horizontal winds is constant with height, in which case the large-scale subsidence, $W = -Dz$; lastly we have assumed that the undulation layer is thin compared with the thickness of the mixed layer.

Given a fixed large-scale environment, a wind field, appropriate values of C_D, and the distribution of sources of s_l and q_t, Eqs. (2) and (3) can be readily integrated if the growth rate of the layer, dh/dt, can be determined. This growth rate can be written as a sum of a diabatic and an adiabatic part:

$$\frac{dh}{dt} = E - Dh, \tag{4}$$

where E denotes the diabatic growth rate and is called the entrainment rate. It represents the rate at which the boundary layer deepens due to mixing processes across the top of the layer. In Eqs. (2) and (3) we see that it is actually E which is most relevant to the budgets of s_l and q_t as h/E can be thought of as a boundary-layer dilution time-scale.

3. Entrainment rules

The discussion of the previous section highlights the role entrainment plays in the evolution of the STBL. It directly determines the depth of the layer (in steady state $h = E/D$ by Eq. (4)), and indirectly the state of the layer. In this section we review different proposals for E. To do so, we reformulate the various proposals in terms of a common framework which helps delineate how different processes are incorporated. To understand and motivate this framework we also spend some time reviewing basic elements of mixed-layer theory for the STBL.

(a) *Framework*

To compare recent proposals for entrainment in stratocumulus-topped mixed layers we express them according to

$$E = \mathfrak{A}\left(\frac{\mathfrak{W}}{\Delta b}\right) + \mathfrak{D}, \tag{5}$$

and evaluate how different proposals imply differing values, or forms, for $\mathfrak{A}$, $\mathfrak{W}$ and $\mathfrak{D}$. Note that our use of the Gothic font is subsequently reserved for terms which are variable in the rule for E. Equation (5) is actually motivated by the form of several of the rules, we adopt it because it nicely partitions various contributions to E according to the values of $\mathfrak{A}$, which can be thought of as an efficiency factor that in general depends on the state; $\mathfrak{W}$, which is a rate of working that depends on the forcing; and $\mathfrak{D}$, a term which represents the effect of non-turbulent processes in deepening the layer; Δb is the isentropic buoyancy difference. The background necessary for thinking about the interpretation of these different terms is developed below.

(i) *Non-turbulent processes and the* $\mathfrak{D}$ *term.* The $\mathfrak{D}$ term has the most ambiguous interpretation, but requires the least theoretical development. In writing Eq. (5) we identify it as a way of incorporating the effect of non-turbulent processes in deepening the entrainment layer. Although, one could argue that it arises in many rules as an artefact of estimating entrainment from large-eddy simulation using budgets over such a layer which can not be easily made to vanish because of undulations in cloud-top height (cf. Moeng and Stevens 1999, also Fig. 1). Nonetheless, a case can be made for including it on physical grounds, in that the radiative cooling of the air just above the inversion, which might be enhanced by moist boundary-layer air which restratifies in (or above) the inversion, could promote a diabatic growth of the layer which $\mathfrak{D}$ attempts to measure. About half of the new generation of rules which we evaluate actually incorporate it.

(ii) *Stratocumulus energetics and the* $\mathfrak{W}$ *term.* By definition, stratocumulus energetics are dominated by buoyancy. Thus, to a first approximation, the rate at which the boundary layer is being driven is related to the integrated buoyancy flux, $\langle \mathcal{B} \rangle$, where $\mathcal{B} \equiv (g/T_0)\overline{w'T_v'}$ and $T_v = T(1 + \epsilon_1 q_v - q_l)$ is the virtual temperature. Virtual temperature, and overbars denote averages at a level, primes the deviation of a variable from that average, and vertical velocity is denoted by w. In the expression for the virtual temperature q_v is the specific humidity of the vapour, q_l is the specific humidity of liquid water and $\epsilon_1 = 1/\epsilon - 1 \approx 0.608$, where $\epsilon = R_d/R_v$ is the ratio of the specific gas constants for dry air and water vapour. In uniformly saturated, or unsaturated, layers it is straightforward to linearly relate perturbations in the buoyancy to perturbations in s_l and q_t. Such a relation provides a basis for relating $\mathcal{B} = \overline{w'b'}$ to $\overline{w's_l'}$ and $\overline{w'q_t'}$ respectively:

$$\langle \mathcal{B} \rangle = \frac{g}{T_0} \left\langle \{\beta_{s,m} H(q_\delta) + \beta_{s,d} H(-q_\delta)\} \frac{\overline{w's_l'}}{c_p} + \{\beta_{q,m} H(q_\delta) + \beta_{q,d} H(-q_\delta)\} T_0 \overline{w'q_t'} \right\rangle. \tag{6}$$

In this expression the betas are local efficiencies. For the unsaturated case they are of the order of unity and depend on the composition of the fluid

$$\beta_{s,d} = 1 + \epsilon_1 q_t, \quad \beta_{q,d} = \epsilon_1; \tag{7}$$

for a saturated fluid they are weak functions of the fluid's state:

$$\beta_{s,m} = \frac{1 + (q_*/\epsilon) - q_t + (T_0/\epsilon)\gamma}{1 + (L_v/c_p)\gamma} \approx 0.5 \quad \text{and} \quad \beta_{q,m} = \left(\frac{L_v \beta_{s,m}}{c_p T_0} - 1 \right) \approx 3.5, \tag{8}$$

where $\gamma = \mathrm{d}q_*/\mathrm{d}T$. The relative efficiency in Eq. (6) is selected by Heaviside's function, H, with $q_\delta = q_t - q_*$. Because $\beta_{s,m} \approx 0.5\beta_{s,d}$ fluctuations in s_l are approximately twice as efficient at driving buoyancy fluctuations in dry air as in cloudy air. Moisture fluctuations, on the other hand, are nearly an order of magnitude more effective in driving buoyancy fluctuations in the cloud layer.

If the forcing varies on a time-scale that is long compared with a turnover time-scale one can expect the layer to be in a quasi-steady state, wherein the shapes of the profiles of s_l and q_t are stationary. In the absence of forcings acting on the interior of the layer, such a constraint forces the fluxes $\overline{w's_l'}$ and $\overline{w'q_t'}$ to be nearly linear. In this case the integration of Eq. (6) across the mixed layer can be performed analytically, allowing us to express the vertically averaged buoyancy flux in terms of boundary forcings:

$$\langle \mathcal{B} \rangle = \tfrac{1}{2}(\eta_{q,0}\mathcal{B}_{q,0} + \eta_{s,0}\mathcal{B}_{s,0} + \eta_{q,h}\mathcal{B}_{q,h} + \eta_{s,h}\mathcal{B}_{s,h}). \tag{9}$$

Here

$$\mathcal{B}_s \equiv \frac{g}{c_p T_0} \overline{w's_l'} \quad \text{and} \quad \mathcal{B}_q \equiv g\overline{w'q_t'} \tag{10}$$

are just the fluxes of s_l and q_t in buoyancy-flux units (e.g. $\mathcal{B}_{s,0}$ is the surface flux of s_l in buoyancy-flux units) and the η terms are global efficiencies which account for the relative depth of the cloud layer in weighting the local (β) efficiencies:

$$\eta_{x,0} = \beta_{x,d}(2\zeta - \zeta^2) + \beta_{x,m}(1 - 2\zeta + \zeta^2) \quad \text{and} \quad \eta_{x,h} = \beta_{x,d}\zeta^2 + \beta_{x,m}(1 - \zeta^2). \tag{11}$$

Here subscript x above can be either a q for moisture, or s for liquid-water static energy and $\zeta = z_b/h$ is the non-dimensional depth of the sub-cloud layer. Equation (9) describes how, in the absence of diabatic terms, the integrated rate of working can be

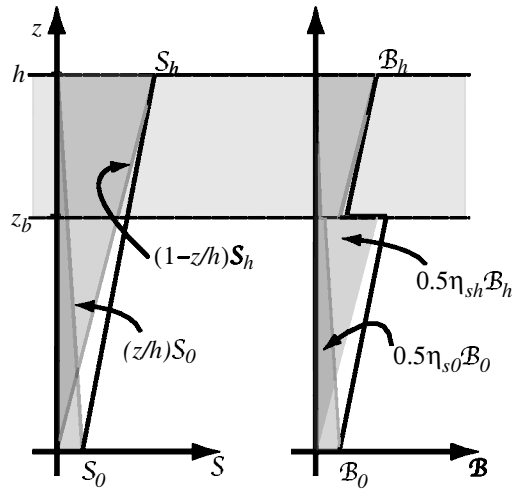

Figure 2. Schematic showing the decomposition of the liquid-water static energy flux $\overline{w's_l'}$ into a top-down and bottom-up component and the implied buoyancy flux. The integrated buoyancy flux in the right panel is given by $\langle \mathcal{B} \rangle = (\eta_{s,0}\mathcal{B}_{s,0} + \eta_{s,h}\mathcal{B}_{s,h})/2$, and is, thus, the sum of the weighted bottom-up and top-down components. See text for description of symbols.

related to boundary fluxes of state variables. It is illustrated schematically in Fig. 2 for the case where $\overline{w'q_t'}$ vanishes.

Above, we considered the energetics of adiabatic layers with fixed boundary forcings. Fixing the boundary fluxes illustrates basic principles but is unrealistic. Indeed, the whole point of an entrainment rule is to allow one to determine the fluxes at the upper boundary which are consistent with the internal dynamics, nominal state and external forcing of the layer. Moreover, because in practice the external forcing (which is dominantly radiative cooling at cloud top) is predominantly diabatic, diabatic processes must be incorporated into the analysis. The simplest way to do this is to confine the forcing to the undulation layer. In this case a budget of the undulation layer allows us to express the boundary fluxes as

$$\mathcal{B}_{s,h} = \frac{g}{c_p T_0}\left(\Delta \mathcal{F}_s - E\,\Delta s_l\right) \tag{12}$$

$$\mathcal{B}_{q,h} = g(\Delta \mathcal{F}_q - E\,\Delta q_t), \tag{13}$$

where Δ denotes a difference across the undulation layer. Writing things in this manner does not preclude the forcing from happening entirely in the cloud layer, as we define h to be below the lowest cloud tops. In the case where it makes sense to think of the forcings as being confined to the cloud tops, the approximation that leads to the above equation is just that the forcings are confined to a layer near cloud top which is thin compared with Δz which is in turn thin compared with h, the first being the more limiting assumption.

Of course, one could allow $\mathcal{F}_s$ and $\mathcal{F}_q$ to diverge below h, but to do so and still estimate $\langle \mathcal{B} \rangle$ as a function of the boundary forcings requires an assumption about the flux profile within the mixed layer. While making such assumptions might lead to results which are quantitatively more realistic (particularly for thin clouds in shallow boundary layers), the additional realism comes at the cost of additional complications. For our purposes of evaluating the impact of different proposals for entrainment the

increased realism does not warrant the additional complications, and so we focus on the more idealized scenario. For similar reasons, while our arguments illustrate a way of incorporating drizzle consistently into the turbulent dynamics, we do not concentrate on such effects here. This simplification allows us to neglect $\mathcal{F}_q$ and associate $\Delta\mathcal{F}_s$ with the radiative flux jump ΔF.

Limiting ourselves to radiative forcings, which we idealize as operating in an arbitrarily thin layer at cloud top, motivates the introduction of yet another symbol:

$$\mathcal{B}_{\Delta F} = \frac{g}{c_p T_0}\Delta\mathcal{F}_s. \tag{14}$$

It captures the contribution to $\mathcal{B}_{s,h}$ from radiative processes at cloud top, and corresponds to the flux we would expect at cloud top in the absence of entrainment. It turns out to be an important term in many attempts to deduce $\mathfrak{W}$. Thus, in scenarios where a radiative forcing $\Delta\mathcal{F}_s = \Delta F$ is confined to the cloudy portions of a thin undulation layer one can estimate the integrated buoyancy flux as

$$\langle\mathcal{B}\rangle = \frac{1}{2}\left\{\eta_{q,0}\mathcal{B}_{q,0} + \eta_{s,0}\mathcal{B}_{s,0} + \eta_{s,h}\mathcal{B}_{\Delta F,h} - E\left(\eta_{q,h} g\Delta q_{\mathrm{t}} + \eta_{s,h}\frac{g}{c_p T_0}\Delta s_{\mathrm{l}}\right)\right\}. \tag{15}$$

Note that in the special case when E is zero $\langle\mathcal{B}\rangle$ depends exclusively on the surface and radiative forcings, and not on the properties of the entrainment interface (as measured by Δs_{l} and Δq).

Casting the various proposals for entrainment in the form given by Eq. (5) is motivated by a desire to separate the forcing of the layer from the state of the layer as manifest in quantities such as Δs_{l} or Δq_{t}. Attempts to relate $\mathfrak{W}$ to $\langle\mathcal{B}\rangle$ fail to do this because $\langle\mathcal{B}\rangle$ depends on E, Δs_{l} and Δq_{t}. To avoid this ambiguity we project any dependency on state-dependent terms in the forcing onto the efficiency terms. So doing, simplifies the forcing term (it results in most rules having a rate of working which is given by $\mathfrak{W} \propto \langle\mathcal{B}\rangle|_{E=0}$) but complicates the efficiency term. We elaborate on this further after we introduce some concepts and terminology which help us evaluate the state of the undulation layer.

(iii) *Layer stability Δb and the $\mathfrak{A}$ term.* In the context of the dry atmospheric boundary layer, where $\mathfrak{D} = 0$, Eq. (5) can be interpreted as saying that a fraction $\mathfrak{A}$ of the energy available to drive turbulence is used to do work against stratification, thereby increasing the potential energy of the system. In cloudy boundary layers the energetics are more complicated. Whereas in the dry boundary layer the change in potential energy of a layer that grows an amount δz is simply $(\Delta b)\delta z$, in cloud-topped systems the growth of the layer generally implies net evaporation or condensation of the cloud layer. Thus, the change in the potential energy of the system depends not only on Δb, but also on the extent to which the cloud layer deepens or shallows for an infinitesimal amount of growth.

Net evaporation of the cloud layer can be thought of as an additional source of energy which can be used to do work on the free troposphere—in effect weakening the stratification at the interface. Some authors have suggested that such effects may be sufficiently strong as to render the interface unstable to mixing processes. This hypothetical process and its variants (e.g. Kraus 1963; Lilly 1968; Deardorff 1980; Randall 1980; MacVean and Mason 1990; Duynkerke 1993) has come to be known as CTEI. It has often been invoked as a mechanism for breaking up stratiform cloud decks. Because varied interpretations of mixing processes at the cloud-top interface lead to

varied formulations for the efficiency parameter $\mathfrak{A}$ it proves useful to review the basis for these varied interpretations.

The starting point for measuring the stratification across the undulation layer is the isentropic buoyancy jump, Δb, which appears in Eq. (5). It can be written as

$$\Delta b = \frac{g}{T_0}\Delta T_{\rm v} = \delta_{\rm d} b - g\beta_{\rm l} q_{\rm l,max}, \tag{16}$$

where

$$\delta_{\rm d} b = \frac{g}{T_0}\left(\beta_{s,{\rm d}}\frac{\Delta s_{\rm l}}{c_p} + \beta_{q,{\rm d}} T_0 \Delta q_{\rm t}\right), \tag{17}$$

is the stability a layer would have in the absence of condensate and

$$\beta_{\rm l} \equiv \frac{L}{c_p T_0}\beta_{s,{\rm d}} - 1/\epsilon \tag{18}$$

accounts for the enthalpy of the condensate when the lower layer (at z_-) is saturated. Here $q_{\rm l,max}$ is the liquid water content at the top of this lower layer and is uniquely determined by the state of that layer. Recall that Δ has a precise meaning, namely the difference in a quantity across the undulation layer. In contrast, we use δ_x to denote the change in buoyancy associated with perturbations of cloud-top parcels by an amount $\Delta s_{\rm l}$ and $\Delta q_{\rm t}$ and in accord with a hypothetical process, x. Above $\delta_{\rm d} b$ denotes a dry, or unsaturated process. Similarly, we can define $\delta_{\rm m} b$ to denote the buoyancy perturbation one would expect in a moist (i.e. saturated) process:

$$\delta_{\rm m} b = \frac{g}{T_0}\left(\beta_{s,{\rm m}}\frac{\Delta s_{\rm l}}{c_p} + \beta_{q,{\rm m}} T_0 \Delta q_{\rm t}\right). \tag{19}$$

The saturated buoyancy perturbation measure has generated wide interest because $\delta_{\rm m} b < 0$ implies that ideal mixtures of mixed-layer air with vanishingly small amounts of free-tropospheric air will be negatively buoyant. For this reason $\delta_{\rm m} b$ is sometimes called the buoyancy reversal parameter, as $\delta_{\rm m} b < 0$ implies the potential for buoyancy reversal. Because some of the studies cited above associate CTEI with this boundary, buoyancy reversal and CTEI are often thought of synonymously, but this is probably not a good idea.

These buoyancy measures are illustrated in Fig. 3. Because whether a process is saturated or dry depends on the relative mixing fraction, this figure examines the buoyancy perturbations as a function of mixing fraction for a case where buoyancy reversal exists. So doing introduces two other measures of the stability of the undulation layer, b_* and χ_*. The first, b_*, defines the most negatively buoyant mixture. It corresponds to a mixture which is just saturated, which (as can be derived from geometrical considerations in Fig. 3) occurs at mixing fraction

$$\chi_* = g\frac{q_{\rm l}\beta_{\rm l}}{\delta_{\rm d} b - \delta_{\rm m} b}. \tag{20}$$

These measures of buoyancy help quantify the relationship between Δb, $\Delta s_{\rm l}$, $\Delta q_{\rm t}$ and $q_{\rm l}$. In dry layers Δb is linearly related to $\Delta s_{\rm l}$ through the factor $g/(c_p T_0)$. To express this relationship more generally we introduce the dimensionless factor

$$\Psi \equiv \frac{c_p \Delta b}{(g/T_0)\Delta s_{\rm l}} = \beta_{s,{\rm d}} + \beta_{q,{\rm d}} c_p T_0 \frac{\Delta q_{\rm t}}{\Delta s_{\rm l}} - \beta_{\rm l} c_p T_0 \frac{q_{\rm l,max}}{\Delta s_{\rm l}}, \tag{21}$$

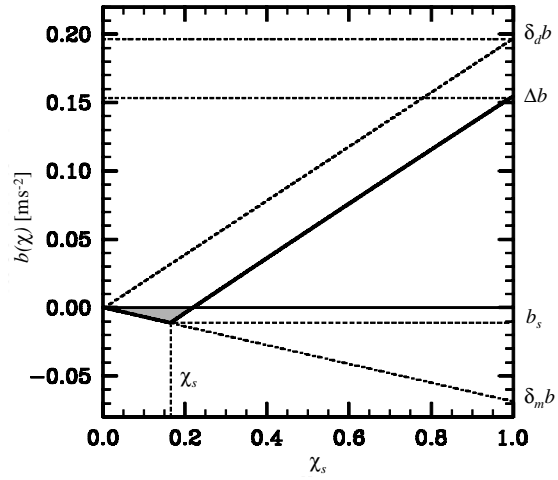

Figure 3. Illustration of the buoyancy of mixtures of air as a function of mixing fraction, χ. Region in which mixtures are negatively buoyant is shaded. See text for further explanation.

which is approximately unity for unsaturated fluids and decreases as moisture effects become more dominant. For many situations in which stratocumulus predominate Δs_{l} is large compared with both $Lq_{\mathrm{l,max}}$ and $c_p T_0 \Delta q_{\mathrm{t}}$ and so Ψ tends to be of the order of unity. Taking it to be constant shall later prove to be a useful approximation in our analysis of the stratocumulus-layer energetics.

(*b*) *Entrainment rules*

Before delving into the specifics of the various rules it is instructive to first evaluate how our desire to develop an explicit equation for E can distort the interpretation of parametrizations in which E is given implicitly. To see this, consider two parametrizations: one given by $E\Delta b = \mathfrak{A}_1 \langle \mathcal{B} \rangle$, the other given by $E\Delta b = \mathfrak{A}_2 \langle \mathcal{B} \rangle_{E=0}$, where both $\mathfrak{A}_1$ and $\mathfrak{A}_2$ are specified as constant. The first parametrization is an implicit equation for E because in general $\langle \mathcal{B} \rangle$ depends on E. Unravelling this implicit dependence by solving explicitly for E results in an equation of the form:

$$E\Delta b = \frac{\mathfrak{A}_1 \langle \mathcal{B} \rangle_{E=0}}{1 + \mathfrak{A}_1 \mu}, \tag{22}$$

where

$$\mu = \left(\eta_{q,h} \frac{g\Delta q_{\mathrm{t}}}{\Delta b} + \frac{\eta_{s,h}}{\Psi} \right) = \frac{\delta_{\mathrm{d}} b}{\Delta b} \zeta^2 + \frac{\delta_{\mathrm{m}} b}{\Delta b} (1 - \zeta^2) \tag{23}$$

measures the importance of top-down turbulent fluxes to the net energetics. Note that if the cloud extends to the surface, $\zeta = 0$ and $\mu = \delta_{\mathrm{m}} b / \Delta b$.

For the most part we expect μ to be greater than zero (and $1 + \mathfrak{A}_1 \mu > 1$), which is another way of saying that $\langle \mathcal{B} \rangle_{E=0}$ overestimates the rate of working relative to $\langle \mathcal{B} \rangle$. In some cases, notably when Δq_{t} is sufficiently negative for buoyancy reversal to occur and the cloud layer is sufficiently deep, then μ will become negative, which means that entrainment fluxes contribute positively to the energetics of the flow. In this situation $\langle \mathcal{B} \rangle_{E=0}$ underestimates the rate of working relative to $\langle \mathcal{B} \rangle$, and hence $1 + \mathfrak{A}_1 \mu$ must be less than one. If the effect is sufficiently strong Eq. (22) can become singular—which can be interpreted as a sort of implied (albeit stricter) CTEI limit. Note that

parametrizations written in terms of the net-forcing tend to manifest some form of a CTEI singularity.

To write Eq. (22) in the form of Eq. (5) requires that the $1 + \mathfrak{A}_1\mu$ term be subsumed in either the rate of working or the efficiency term. We do the latter. Although our choice is arbitrary, it does considerably simplify the subsequent analysis as it forces most of the parametrizations we consider to represent their rate of working as

$$\mathfrak{W} = 2\langle\mathcal{B}\rangle_{E=0} = \eta_{q,0}\mathcal{B}_{q,0} + \eta_{s,0}\mathcal{B}_{s,0} + \eta_{s,h}\mathcal{B}_{\Delta F,h}, \tag{24}$$

where the factor of two cancels the factor of $1/2$ in Eq. (9). Defining $\mathfrak{W}$ in this manner projects most of the differences among parametrizations on to either the $\mathfrak{A}$ or the $\mathfrak{D}$ term.

(i) *AL (Lock 1998).* The first parametrization we examine is one proposed by Lock (1998). It was derived on the basis of a number of large-eddy simulations, wherein entrainment was found to be well described by Eq. (5) if $\mathfrak{W}$ is given by Eq. (24),

$$\mathfrak{A} = \mathfrak{A}_{\rm AL} = 0.23 \quad \text{and} \quad \mathfrak{D} = \mathfrak{D}_{\rm AL} = \alpha\beta_{s,\rm m}\frac{\mathcal{B}_{\Delta F,h}}{\Delta b}. \tag{25}$$

In the $\mathfrak{D}$ term

$$\alpha = 1 - \exp(-b_1\mathcal{L}) \quad \text{and} \quad b_1 = \kappa\left(\frac{(h\mathfrak{W})^{2/3}}{z_{\rm c}\Delta b}\right), \tag{26}$$

where $\mathcal{L} = \int_0^h \rho q_{\rm l}\,{\rm d}z$ is the liquid-water path, b_1 is an absorption coefficient, κ, weighted by the ratio of the cloud-top undulation height $\Delta z_p = \{(h\mathfrak{W})^{2/3}/\Delta b\}$ to the cloud depth $z_{\rm c}$, which, thus, estimates the liquid water in the undulations. For Lock's simulations κ was generally set to 156 $\rm m^2 kg^{-1}$, and the undulations tended to be 10 to 20% of the cloud depth, whereby $b_1 \approx 15$.

In the presence of buoyancy reversal ($\delta_{\rm m}b < 0$) Lock found that the above relation did not fit the simulations well. To better fit the simulations he suggested modifying the rate of working and direct terms so that

$$\mathfrak{W} = \mathfrak{W}^*_{\rm AL} = \eta_{q,0}|_{\zeta=1}\mathcal{B}_{q,0} + \eta_{s,0}|_{\zeta=1}\mathcal{B}_{s,0} + \eta_{s,h}|_{\zeta=1}\mathcal{B}_{\Delta F} + 0.24\chi_*\frac{-b_*}{h\Delta b}(z_{\rm c}\Delta b)^{3/2} \tag{27}$$

$$\mathfrak{D} = \mathfrak{D}^*_{\rm AL} = \beta_{s,\rm m}\frac{\mathcal{B}_{\Delta F,h}}{\Delta b}. \tag{28}$$

The modification to $\mathfrak{W}$ amounts to assuming that the layer energetics are consistent with what one would expect in a uniformly unsaturated layer ($\zeta = 1$) with an additional forcing associated with buoyancy reversal. In addition, $\mathfrak{D}$ is enhanced by neglecting the effect of α.

These changes greatly enhance the efficiency with which radiation is allowed to generate turbulence in the cloud layer, and are justified quasi-empirically (i.e. on the basis of simulations). However, because Lock's simulation in the buoyancy reversal regime evolved so rapidly, and some critical terms (such as effective liquid-water content) were not possible to evaluate objectively, the goodness of fit was difficult to evaluate. The proposal also lacks credibility because $\mathfrak{D}_{\rm AL} \neq \mathfrak{D}^*_{\rm AL}$ and $\mathfrak{W}_{\rm AL} \neq \mathfrak{W}^*_{\rm AL}$ for $\delta_{\rm m}b = 0$. For these reasons our subsequent work will focus on Lock's suggested rule for regimes *without* buoyancy reversal—even in regimes for which it was not designed, i.e. for $\delta_{\rm m}b < 0$.

(ii) *NT (Turton and Nicholls 1987).* When written as follows

$$E = a_1 \frac{w_*^3}{h\delta_{\rm NT} b} \quad \text{where} \quad \delta_{\rm NT} b = \frac{\Delta b}{1 + a_2\{1 - (\Delta_{\rm m}/\Delta b)\}} \quad \text{and} \quad a_2 = 60 \tag{29}$$

the NT rule is very similar to Eq. (5). The main differences are that $w_* \equiv 2.5h\langle \mathcal{B} \rangle$ is proportional to the net forcing, and the effective stratification of the interface is measured by an ad hoc buoyancy difference $\delta_{\rm NT} b$. This latter term goes to $\Delta b/(1 + a_2)$ as $\Delta_{\rm m}$ goes to zero, where $\Delta_{\rm m}$ measures the integrated buoyancy excess

$$\Delta_{\rm m} = 2 \int_0^1 b(\chi)\, {\rm d}\chi,$$

$b(\chi)$ is the buoyancy excess, relative to air at z_{i^-}, of a mixture of $(1 - \chi)$ parts boundary-layer air with χ parts free-tropospheric air. From Fig. 3 we note that

$$\Delta_{\rm m} = \delta_{\rm d} b + \chi_*(\delta_{\rm m} b - \delta_{\rm d} b)(2 - \chi_*) \tag{30}$$

$$= \delta_{\rm d} b - g\beta_{\rm l} q_{\rm l} \left(2 - \frac{g\beta_{\rm l} q_{\rm l}}{\delta_{\rm d} b - \delta_{\rm m} b}\right). \tag{31}$$

Taking $a_1 = 0.2$ as was recommended by NT, we can relate Eq. (29) to (5) by again specifying $\mathfrak{W}$ as per Eq. (24), but this time taking

$$\mathfrak{A} = \mathfrak{A}_{\rm NT} = \frac{1 + a_2\{1 - (\Delta_{\rm m}/\Delta b)\}}{4 + [1 + a_2\{1 - (\Delta_{\rm m}/\Delta b)\}]\mu} \tag{32}$$

and setting $\mathfrak{D} = 0$.

(iii) *RK (Konor and Arakawa 2001).* Randall (personal communication, 2001) has been experimenting with a new entrainment rule which is described by Konor and Arakawa. This scheme is prognostic, in the sense that E is not related directly to the forcings, but rather to the time-resolved energetics of the layer as measured by the turbulent kinetic energy e:

$$E = \frac{2ae^{3/2} + \beta(gh/T_0)(\Delta F/\rho c_p)}{a' e^{1/2} + h\delta_{\rm m} b}, \tag{33}$$

where $a = 0.25$ and $a' = 1.25$. For the cases we consider here $\delta_{\rm m} b$ is generally much greater than $e^{1/2}/(a_2 h)$ thus the additional factor of e in the denominator can be considered negligible. Its main purpose is to allow the parametrization to be well behaved in the neutral $\delta_{\rm m} b = 0$ limit.

In buoyancy-driven layers the dissipation is defined such that $\varepsilon = \langle \mathcal{B} \rangle = e^{3/2}/(c_\varepsilon h)$ where the constant c_ε is of the order of unity. For simplicity, and to satisfy the entrainment rule for the dry convective boundary layer given recommended values for a and a', we set $c_\varepsilon = 1$. Substituting for e in the numerator of Eq. (33) and neglecting the factor of e in the denominator yields a diagnostic version for E which can be cast into the desired form with $\mathfrak{W}$ given by Eq. (24),

$$\mathfrak{A} = \mathfrak{A}_{\rm RK} = \frac{a}{(\delta_{\rm m} b/\Delta b) + a\mu} \quad \text{and} \quad \mathfrak{D} = \mathfrak{D}_{\rm RK} = \beta_{s,{\rm m}} \frac{\mathcal{B}_{\Delta F, h}}{\delta_{\rm m} b}. \tag{34}$$

As was the case for the NT parametrization, representing the entrainment as proportional to the net forcing leads to the μ term in the definition of $\mathfrak{A}$. This provides an additional pathway for buoyancy reversal to influence E.

(iv) *CM (Moeng 2000).* Like Lock, Moeng used LES as a way to calibrate an entrainment rule. The form which she advocates was initially written as follows:

$$E = \frac{0.2(\rho_0 \overline{w's'_{10}} + 2.5\Delta F)}{\rho_0 \Delta s_1} + \frac{2\Delta F}{\rho_0 \Delta s_1}\{1 - \exp(-\sqrt{b_m \mathcal{L}})\}, \tag{35}$$

where $b_m = 0.9\ \mathrm{m^2 kg^{-1}}$ is a constant, thus allowing the undulation term to be expressed in terms of bulk quantities.

Moeng uses s_l in both the denominator and the surface forcing component of her parametrization. To recast her equation in the form given by Eq. (5) requires that we absorb the difference between Δs_l and Δb in the definition of the efficiency parameter $\mathfrak{A}$, (making use of the definition of Ψ from Eq. (21)). So doing allows us to express Eq. (35) in the form of Eq. (5) if we define:

$$\mathfrak{W} = \mathfrak{W}_{\mathrm{CM}} = \mathcal{B}_{s,0} + 2.5\mathcal{B}_{\Delta F,h}, \tag{36}$$

and

$$\mathfrak{A} = \mathfrak{A}_{\mathrm{CM}} = 0.2\Psi \quad \text{and} \quad \mathfrak{D} = \mathfrak{D}_{\mathrm{CM}} = \alpha \frac{\mathcal{B}_{\Delta F,h}}{\Delta b} \tag{37}$$

where in $\mathfrak{D}_{\mathrm{CM}}$

$$\alpha = 10\mathfrak{A}\{1 - \exp(-\sqrt{b_m \mathcal{L}})\}. \tag{38}$$

Note that the partitioning of Moeng's parametrization between the $\mathfrak{D}$ and $\mathfrak{W}$ terms reflects her motivation for the respective terms, for instance her choice of b_m reflects an assumption about the scale length of the interface. Also, her formulation for $\mathfrak{W}$ does not follow Eq. (24) but has a more empirical flavour, which allows no role for moisture fluxes.

(v) *DL (Lilly 2002).* The last modern entrainment parametrization of which we are aware is a recent proposal by Lilly. It is also based on the set of simulations used by Moeng to calibrate her parametrization. Like Moeng, Lilly chooses $\mathfrak{W}$ more empirically, more strongly weighting cloud-top fluxes. Like Nicholls and Turton, he defines an effective buoyancy at cloud top which attempts to account for buoyancy reversal in some weighted sense.

Lilly proposes that entrainment acts to ensure that

$$\mathcal{B}_h = -A_n \langle \sigma^n \mathcal{B} \rangle, \tag{39}$$

where A_n is universal and $\sigma \equiv z/h$, retains its prior meaning. Note that in the special case where $n = 0$, $B_h = -E\Delta b$, Eq. (39) is identical to Eq. (5) with $\mathfrak{D} = 0$. In the case when $n \neq 0$ one can view Eq. (39) as a generalization of the previous approach where the σ^n terms modify the relative efficiency of the top-down versus bottom-up component of the buoyancy flux:

$$\langle \sigma^n \mathcal{B} \rangle = \frac{[\widehat{\eta}_{q,0}\mathcal{B}_{q,0} + \widehat{\eta}_{s,0}\mathcal{B}_{s,0} + \widehat{\eta}_{s,h}\mathcal{B}_{\Delta F,h} - ghE\{\widehat{\eta}_{s,h}(\Delta s_l/c_p T_0) + \widehat{\eta}_{q,h}\Delta q_t\}]}{(n+2)(n+1)}. \tag{40}$$

Here

$$\widehat{\eta}_{x,0} = \beta_{x,\mathrm{d}}\{(n+2)\zeta^{n+1} - (n+1)\zeta^{n+2}\} + \beta_{x,\mathrm{m}}\{1 - (n+2)\zeta^{n+1} - (n+1)\zeta^{n+2}\} \tag{41}$$

$$\widehat{\eta}_{x,h} = (n+1)\{\beta_{x,\mathrm{d}}\zeta^{n+2} + \beta_{x,\mathrm{m}}(1 - \zeta^{n+2})\} \tag{42}$$

are modified efficiencies which account for the preferential weighting of cloud-top processes.

To write Eq. (39) in the form of an entrainment rate requires that B_h be related to E. As noted above this is usually done by taking

$$\mathcal{B}_h = -E\delta b, \tag{43}$$

where δb is some measure of the strength of the undulation-layer stability, a measure which we have seen varies considerably among different entrainment proposals, with Δb and $\delta_{\rm m} b$ being two limits. Given Eq. (39), Lilly argues that the more general relation

$$\delta b = \delta_{\rm DL} b \equiv \{(1-\alpha_{\rm l})\delta_{\rm d} b + \alpha_{\rm l}\delta_{\rm m} b\}, \tag{44}$$

where

$$\alpha_{\rm l} = \frac{\tanh(a_{\rm l}\chi_s)}{\tanh(a_{\rm l})} \tag{45}$$

is a variable wetness factor which takes values between zero and one, and is tuned via the factor $a_{\rm l}$ which following Lilly we set to 2.45.

These arguments can be used above to transform a relation of the form of Eq. (39) into the form of Eq. (5). To do so we define $\mathfrak{W}$ following Eq. (24) except that the efficiency terms, η, are replaced by modified efficiencies, $\widehat{\eta}$, given above, and

$$\mathfrak{A} = \mathfrak{A}_{\rm DL} = \frac{A_n(\delta_{\rm DL} b/\Delta b)}{1 + A_n(\delta_{\rm DL} b/\Delta b)\widehat{\mu}} \tag{46}$$

and $\mathfrak{D} = 0$. Note that in the definition of $\mathfrak{A}_{\rm DL}$ the $\widehat{\mu}$ term is equivalent to μ as defined in Eq. (23) except that again the efficiencies η are replaced by the modified efficiencies $\widehat{\eta}$. Also following Lilly, A_n and n are set to values of 3 and 1, respectively*.

For the case $n = 0$ Lilly's parametrization differs from that of Nicholls and Turton only in terms of how he defines the buoyancy of the interface. By weighting the buoyancy integral more strongly for cloud-top processes, Lilly accentuates the forcing from radiative cooling at cloud top and amplifies the effect of thermodynamic fluxes associated with entrainment. To get a sense of how this weighting changes the relative contributions of different driving fluxes to the integral forcing one can examine $\eta_{x,h}/\eta_{x,0}$ and $\widehat{\eta}_{x,h}/\widehat{\eta}_{x,0}$ as a function of ζ, where subscript x can either be s or q. So doing shows that the weighting favours buoyancy production by top-down moisture fluxes in cloud layers which are relatively thin (approximately 15% of the layer depth). The boost that this approach gives to cloud-top fluxes of moisture might be expected to accelerate the dissipation of the cloud layer in many cases.

(vi) *Historical proposals.* Equation (5) represents a way of thinking which describes most recent entrainment rules. In contrast, previous rules tended to focus on diagnosing entrainment by imposing a constraint on the buoyancy flux $\mathcal{B}$. For instance, one can define a quantity,

$$\mathcal{I} \equiv -\frac{\int_0^h \mathcal{B}H(-\mathcal{B})\,{\rm d}z}{\int_0^h \mathcal{B}H(\mathcal{B})\,{\rm d}z} \tag{47}$$

which measures the area of the negative buoyancy flux in the mean profile relative to the positive area. Kraus and Schaller (1978) proposed to diagnose the entrainment rate

* These values lead to slightly worse fits to the data of Moeng than is reported by Lilly. These differences arise because Lilly optimized his wetness based on a slightly different characterization of Moeng's simulation than she reported.

TABLE 1. ENTRAINMENT TEST CASES DERIVED FROM MOENG (2000), LOCK (1998) AND NICHOLLS AND LEIGHTON (1986)

Case	ΔF	$\rho(\overline{w's'_{10}})$	$\rho L_v(\overline{w'q'_{t0}})$	z_i	z_c	$\Delta s_l/c_p$	Δq_t	$q_{l,max}$	$\mathcal{L}$
Moeng 02	74	1	26	928	510	3.7	−1.4	0.55	114
Moeng 04	74	1	28	812	487	4.7	−1.4	0.52	93
Moeng 07	111	1	32	765	474	7.3	−3.1	0.41	65
Moeng 10	74	50	84	750	524	6.3	−3.4	0.22	33
Moeng 14	74	1	30	750	487	7.1	−3.1	0.36	53
Moeng 17	74	1	39	713	513	10.5	−6.6	0.23	26
Lock Ea	60	0	0	798	450	2.6	−1.0	0.62	119
Lock Ec	60	0	0	745	400	2.7	−0.9	0.59	112
Lock Ed	60	0	0	748	210	4.0	−1.7	1.00	296
NT 620	50	0	0	700	360	9.0	−3.0	0.54	101
NT 624	66	12	50	1120	580	9.7	−3.6	0.84	238

See text and Table A.1 for explanation of symbols.

as that value of E for which $\mathcal{I} = 0.2$. A related, but somewhat earlier proposal was the basis of the analysis by Schubert *et al.* (1979a). In their proposal they chose E such that

$$\mathcal{B}_{\min} = -\frac{1-k}{2k}\langle \mathcal{B} \rangle, \tag{48}$$

with $k = 0.2$. While these rules are of historic interest, and are useful benchmarks, our focus will be on the types of rules which can be described by Eq. (5).

(c) *Test cases*

To both test our implementation of the various entrainment rules, and gain insight into the range of behaviour they exhibit, we first evaluate their predictions for E for a suite of 11 nocturnal test cases culled from the literature and tabulated in Table 1. Most of these test cases are from simulations by Lock (1998) and Moeng (2000); the two exceptions, NT620 and NT624, are drawn from the analysis of nocturnal flight data by Nicholls and Leighton (1986). With the exception of cases Moeng 10 and 17, all of the cases are stable by the CTEI criterion of Randall (1980) and Deardorff (1980).

Our suite of test cases focuses on cases with near-uniform cloud cover, furthermore our tests use the published values of z_c, q_l and $\mathcal{L}$, and a fixed air density of 1 g kg^{-1}, rather than values produced by a mixed-layer state designed to most closely approximate the state of the simulated or observed test case. In addition κ (which appears in the $\mathfrak{D}$ term of the AL and CM rules) was set to 156 g m^{-2} except in Lock's cases Ec and Ed for which it was given the values 40 and 78 g m^{-2} respectively, as used by Lock (1998). The isobaric specific heat, c_{pd} was given a value of 1013 J kg^{-1}. Lastly, in these and all other tests, we impose the specified radiative forcing irrespective of cloud amount. Our motivation for using the published values of $\mathcal{L}$ and z_c rather than those predicted by a mixed-layer model with the same mean state, is that LES is often based on approximate thermodynamic relations, hence it is difficult to maintain consistency between the simulated cloud depth, $q_{l,max}$ and $\mathcal{L}$ and that predicted by a mixed-layer model—even if the simulation is well mixed. The extent to which the layer is not well mixed, and the cloud layer is sub-adiabatic, or the thermodynamic structure is not uniform in the horizontal, further complicates interpretations.

In Table 2 we tabulate E for the test cases as predicted by the various entrainment rules. We also tabulate a further indicator of the entrainment-rule behaviour, which we

TABLE 2. ENTRAINMENT VELOCITIES, E (cm s^{-1}) AND EFFICIENCIES, $\widetilde{\mathfrak{A}}$, AS DEFINED BY EQ. (49)

Case	E	CM	AL	DL	NT	NT ($a_2 = 30$)	RK
Moeng 02	2.70	1.87 (0.68)	1.18 (0.43)	1.84 (0.67)	2.47 (0.90)	1.99 (0.73)	2.84 (1.04)
Moeng 04	1.40	1.41 (0.75)	0.67 (0.36)	1.08 (0.57)	1.48 (0.79)	1.18 (0.62)	1.77 (0.94)
Moeng 07	1.07	1.25 (0.78)	0.46 (0.29)	0.93 (0.58)	1.20 (0.75)	0.87 (0.54)	2.07 (1.29)
Moeng 10	0.87	0.84 (0.70)	0.32 (0.26)	0.77 (0.64)	0.86 (0.72)	0.61 (0.51)	3.09 (2.59)
Moeng 14	0.77	0.82 (0.75)	0.28 (0.26)	0.64 (0.59)	0.81 (0.74)	0.58 (0.53)	1.52 (1.40)
Moeng 17	0.45	0.48 (0.68)	0.16 (0.23)	0.43 (0.61)	0.40 (0.56)	0.28 (0.40)	NaN
Lock Ea	1.88	2.14 (0.49)	2.23 (0.51)	2.32 (0.53)	2.80 (0.64)	2.45 (0.56)	3.49 (0.80)
Lock Ec	1.28	2.07 (0.53)	1.03 (0.26)	1.97 (0.50)	2.54 (0.65)	2.18 (0.56)	3.01 (0.77)
Lock Ed	1.34	1.71 (0.57)	1.04 (0.35)	2.14 (0.71)	2.94 (0.98)	2.37 (0.79)	2.62 (0.87)
NT 620	0.55	0.50 (0.87)	0.14 (0.24)	0.31 (0.54)	0.41 (0.71)	0.29 (0.51)	0.60 (1.05)
NT 624	0.56	0.75 (0.97)	0.34 (0.44)	0.58 (0.76)	0.82 (1.07)	0.61 (0.79)	1.01 (1.31)

The entrainment rate in the first column of data is that estimated either from the simulations themselves or the data. The remaining values are those predicted by the respective entrainment rules. For the Moeng 17 cases the RK rule is unable to derive a physical value of E, and thus is given the value 'NaN' for not a number.

call the effective efficiency $\widetilde{\mathfrak{A}}$ and define as follows:

$$\widetilde{\mathfrak{A}} = E \frac{\Delta b}{\mathcal{B}_{\Delta F, h}}. \tag{49}$$

For any given rule $\widetilde{\mathfrak{A}}$ differs from $\mathfrak{A}$ in that the former accounts for both $\mathfrak{D}$ and sources of turbulence other than radiative fluxes, hence values greater than unity are not forbidden.

The tabulation illustrates that our implementation of the entrainment rules are faithful to the author's definitions. For instance, the correspondence between E as given by the CM rule and the Moeng test cases is commensurate with the results in Moeng (2000) (her Fig. 16). E as given by the NT rule with $a_2 = 60$ is in accord with results described by Turton and Nicholls (1987). Similarly, the behaviour of the AL and DL rules are in accord with the original description of these rules (cf. Lock 1998; Lilly 2002).

The results indicate considerable variability among rules, with the AL rule tending to produce the least entrainment and the RK rule producing the most. The differences are often a factor of two or three, but can be larger. Although there is some grouping of predictions, with the CM, DL and NT rules producing similar values of entrainment, it is still straightforward to find large differences between any two rules. Given that some of the rules were derived using the same set of data, or same technique, this degree of disparity is surprising and somewhat discouraging. Because such a situation could arise from poorly chosen test cases, it makes sense to further evaluate the entrainment rules by examining what steady states they imply given some mean climatological forcings.

4. STEADY-STATE ANALYSIS

Because different proposals for limiting the stratocumulus regime are expected to depend on which entrainment rule one uses, we also evaluate the sensitivity of such proposals to rules for E. Recall that in the introduction we identified three such proposals: CTEI, bulk energetic constraints and drizzle. In the subsequent analysis we focus on the point in parameter space where $\delta_{\mathrm{m}} b = 0$, $\mathcal{I} = \mathcal{I}_{\mathrm{crit}} = 0.1$, or $\mathcal{L} = 0.3$ kg m^{-2} occurs, with these lines being taken as proxies for the potential relevance of these three proposals respectively.

TABLE 3. MODEL PARAMETERS

Parameter	Value
C_D	0.0011
$\|\mathbf{U}\|$	7.0 m s^{-1}
$q_t(z)$	3.5 g kg^{-1}
$s_l(z)$	311 000 $- gz$ J kg^{-1}
c_p	1013 J kg^{-1} K^{-1}

Following Schubert *et al.* (1979a) we focus on steady states as a function of the divergence D and the sea surface temperature (SST). Other parameters in the model are given in Table 3. The state of the free troposphere is based on values taken from the National Centers for Environmental Prediction (NCEP) climatology for a point near the maximum stratocumulus incidence for June through August. This leads to a somewhat warmer free troposphere than that which was used in previous studies which were based on the Oakland sounding, but is more reflective of the heart of the stratocumulus regime. To specify the variation of s_l with height in the free troposphere, i.e. $z > h$, we linearize about the climatological value of s_l near the top of the temperature inversion (which we take at 850 hPa, or 1550 m). Because by definition dT/dz changes sign at this point, such a profile is isothermal.

To facilitate the comparisons we focus on values of $\widetilde{\mathfrak{A}}$ (defined in Eq. (49)) at steady state. To help unravel the meaning of different values of $\widetilde{\mathfrak{A}}$ we first illustrate the behaviour of the mixed-layer model forced by what, following Bretherton and Wyant (1997), we call the minimal model, namely the mixed-layer model as closed by an entrainment rule of the form:

$$E = \mathfrak{A}\left(\frac{\mathcal{B}_{\Delta F,h}}{\Delta b}\right). \tag{50}$$

The idea being that values of $\widetilde{A}$ from steady states of the mixed-layer model closed by more elaborate entrainment rules will be identical to the steady states of the mixed-layer model closed by Eq. (50) so long as $\mathfrak{A} = \widetilde{\mathfrak{A}}$.

(*a*) *Minimal model*

Solutions to Eqs. (2)–(4) closed by Eq. (50) are contoured in Fig. 4, where the three rows of figures correspond to three different combinations of ΔF and $\mathfrak{A}$. From the figure, where only cloudy states are shown, we note some generic features. The left panels show that for the most part, both h and $\mathcal{L}$ deepen as one moves to higher SSTs or lower D. The right column of panels shows that the sensible-heat flux ($\overline{w's'_{l0}}$) tends to decrease and the moisture flux ($\overline{w'q'_{t0}}$) increases, indicating that the mixed layer tends to cool and dry relative to the local sea surface, as one moves to regions of lower D and larger SST. The sensitivities of h and $\overline{w's'_{l0}}$ to the large-scale conditions are rather similar to one another, changing by up to a factor of four across the parameter space and exhibiting marked sensitivity to both D and SST. On the other hand, $\overline{w'q'_{t0}}$ is relatively insensitive to D; as the STBL equilibrium state deepens with decreasing D its moisture content stays relatively fixed. Barring changes in $\langle s_l \rangle$ this would suggest that the relative depth of the cloud layer would be larger, leading to an increase in $\mathcal{L}$, as is indeed evident by the shading in the left-most panels. Hence, the relatively strong dependence of $\mathcal{L}$ on D seems to reflect the insensitivity of $\overline{w'q'_{t0}}$ to D.

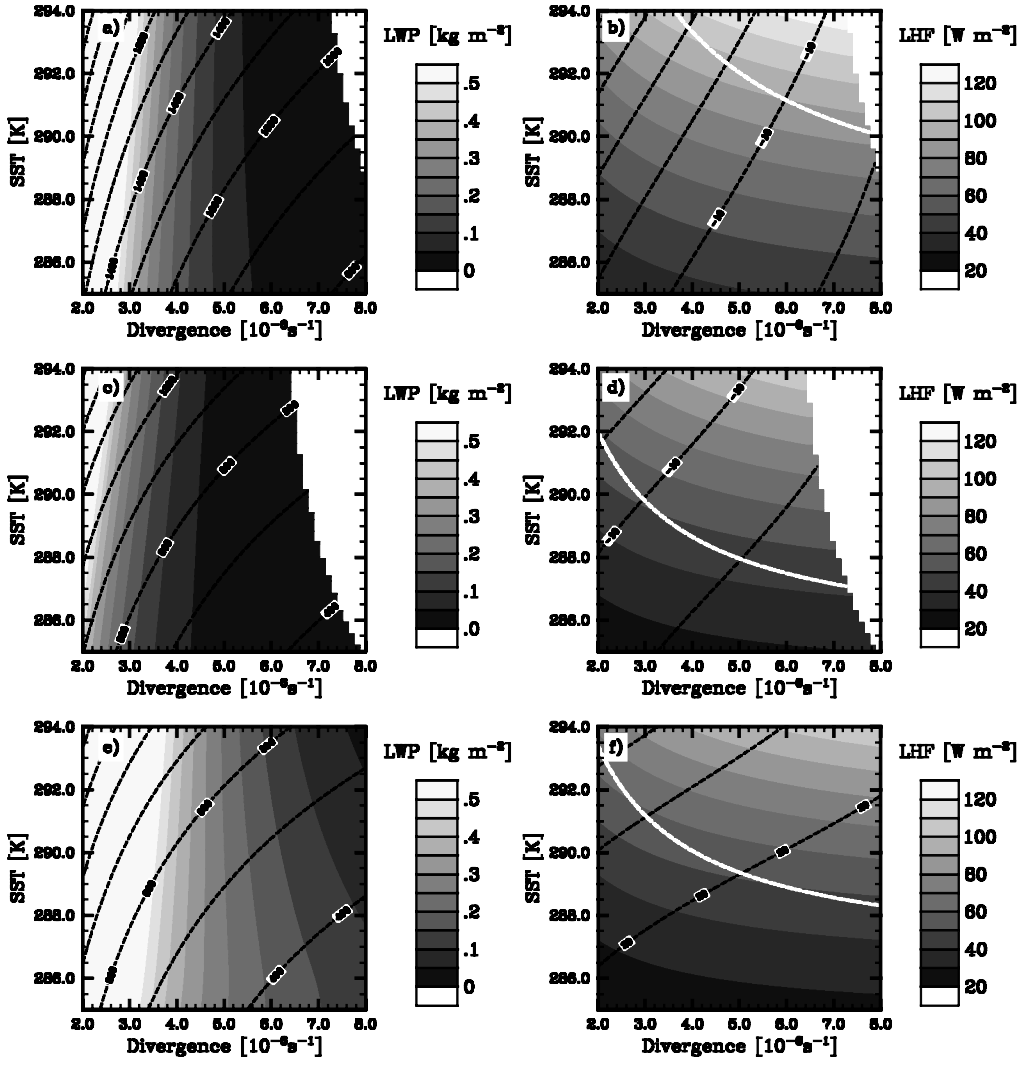

Figure 4. Steady-state solutions as a function of D and sea surface temperature for parameters in Table 3. In the left panels we shade contours of liquid-water path (LWP) and contour boundary-layer depth, h. In the right panels we shade contours of the latent-heat flux (LHF) and contour the sensible-heat flux $\overline{w's'_{10}}$. The buoyancy reversal line $\delta_m b = 0$ is also shown by the white dashed line in the right panels, with regions of buoyancy reversal being above and to the right of this line. In panels (a) and (b) we specify $\Delta F = 60$ W m^{-2}, $\mathfrak{A} = 1$. Panels (c) and (d) are identical to (a) and (b) except for $\Delta F = 30$ W m^{-2}. Panels (e) and (f) are identical to (a) and (b) except that $\mathfrak{A} = 0.5$. See text for further explanation.

The sensitivity of the solutions to the strength of forcing, ΔF, can be evaluated by comparing the first and second rows of panels in Fig. 4. When the radiative forcing is reduced by a factor of two (i.e. in the second row of panels) we find substantially shallower (almost a factor of two) layers and markedly thinner (smaller $\mathcal{L}$) clouds. Overall, the shallowing of the boundary layer reduces the extent in parameter space where cloudy equilibria are found. Surface fluxes are more marginally affected, with latent-heat fluxes becoming somewhat smaller and sensible-heat fluxes somewhat larger as ΔF decreases.

Comparing the first row of panels with the third (which correspond to solutions for $\mathfrak{A}$ halved) illustrates the sensitivity of the equilibria to variations in $\mathfrak{A}$. As far as h is concerned, halving $\mathfrak{A}$ has a commensurate effect to halving the forcing. However, the thermodynamic state of the boundary layer is markedly more sensitive to changes in $\mathfrak{A}$. The substantial increase in $\mathcal{L}$ in panel (e) is accompanied by sensible-heat fluxes which have changed sign in panel (f) relative to those in panels (b) or (c), although changes in q_t as evidenced by changes in $\overline{w'q'_{t0}}$ are relatively modest. For smaller values of $\mathfrak{A}$ one finds not only substantially shallower but also much cooler equilibrium solutions.

In terms of regime boundaries, the dependence of drizzle on $\mathcal{L}$ implies that drizzle will be most sensitive to D. Because $\overline{w's'_{l0}} < 0$ is a necessary (and usually sufficient) condition for the buoyancy flux profile to have any negative area in a steady state, for $\mathfrak{A} = 1$ almost the entire parameter space corresponds to solutions where $\mathcal{I} > \mathcal{I}_{crit}$. For $\mathfrak{A} = 0.5$ we find that, except for very deep cloud layers, $\mathcal{I}$ is less than $\mathcal{I}_{crit}$. The buoyancy reversal regime is most evident where the boundary layer is relatively shallow and warm, i.e. in the upper right of the plots. It depends most strongly on $\mathfrak{A}\Delta F$, and tends to cover more parameter space as either $\mathfrak{A}$ or ΔF decreases.

This behaviour is readily understood with the help of the algebraic solutions to the steady-state mixed-layer model. Writing these in terms of (h, $\overline{w'q'_{t0}}$, $\overline{w's'_{l0}}$) yields:

$$h = \frac{V}{D}\left(\frac{\mathfrak{A}/\Psi}{1 + G\{1 - (\mathfrak{A}/\Psi)\}}\right) \tag{51}$$

$$\overline{w's'_{l0}} = \Delta F\{1 - (\mathfrak{A}/\Psi)\} \tag{52}$$

$$\overline{w'q'_{t0}} = V(q_{t,s} - q_{t,+})\left(\frac{\mathfrak{A}/\Psi}{1 + G}\right), \tag{53}$$

where

$$V = \frac{\Delta F}{(s_{l,+} - s_{l,s})} \quad \text{and} \quad G = \frac{V}{C_D\|\mathbf{U}\|}. \tag{54}$$

The velocity scale V is of the order of $C_D\|\mathbf{U}\|$. Thus, for most of the conditions considered here, both G and Ψ are of the order of unity.

Because in general $s_{l,+}$ depends on h, and Ψ depends on the state of the mixed layer, Eqs. (51)–(53) are implicit. Nonetheless, neglecting the implicit effects in Eqs. (51)–(53) still yields useful insight. Because for ΔF and $s_{l,+}$ fixed, V tends to increase with increasing SST, thus h, and $\overline{w'q'_{t0}}$ should also increase with SST, $\overline{w'q'_{t0}}$ somewhat more strongly because both V and $q_{t,s} - q_{t,+}$ depend on SST. Moreover, while h depends inversely on $\mathfrak{D}$, neglect of implicit terms suggests that $\overline{w'q'_{t0}}$ should be independent of $\mathfrak{D}$, as is roughly the case. Both h and $\overline{w'q'_{t0}}$ scale with the efficiency factor $\mathfrak{A}/\Psi$. From the point of view of the moisture flux this effect is damped by increasingly stable layers (larger G). In terms of h, the stability of the layer can either damp or amplify the $\mathfrak{A}/\Psi$ scaling, depending on the sign of $1 - \mathfrak{A}/\Psi$.

The dependence of $\overline{w's'_{l0}}$ on the large-scale state is more indirect. For $\mathfrak{A}$ small we expect relatively little sensitivity of $\overline{w's'_{l0}}$ to the large-scale conditions (which is indeed the case in panel (f)), while as $\mathfrak{A}$ approaches unity, $\overline{w's'_{l0}}$ will become increasingly sensitive to the effects of SST and $\mathfrak{D}$ on the boundary-layer state as such changes influence Ψ. For $\mathfrak{A} = 1$ changes in Ψ could even be expected to regulate the sign of $\overline{w's'_{l0}}$.

This analysis illustrates that to the extent that previous studies (e.g. Slingo 1980; Klein and Hartmann 1993), have found lower-tropospheric stability (essentially

$s_{l,+} - s_{l,s}$) to be a good predictor of boundary-layer clouds, the effective velocity scale V (and/or G) should be more relevant. The analysis also indicates that equilibrium solutions to the mixed-layer equations should exhibit substantial sensitivity to $\mathfrak{A}$, thus suggesting that the various entrainment rules reviewed in section 3 will have a substantial impact on the steady states of the mixed-layer equations.

(*b*) *Other rules*

As previously discussed, given an equilibrium solution to Eqs. (2)–(4) closed by some other entrainment rule, we can interpret it in the light of the previous analysis by comparing the efficiencies as measured by $\widetilde{\mathfrak{A}}$, where $\widetilde{\mathfrak{A}}$ is given in Eq. (49). Results from this analysis are presented in Fig. 5, which demonstrates that the steady states of Eqs. (2)–(4) are remarkably sensitive to the variety of entrainment rules existing in the literature. In the centre of the parameter space values of $\widetilde{\mathfrak{A}}$ vary by more than a factor of 3, from $\widetilde{\mathfrak{A}} \approx 0.45$ for the AL rule to $\widetilde{\mathfrak{A}} \approx 1.5$ for the RK rule. Not only do the values of $\widetilde{\mathfrak{A}}$ vary among rules, but the variability of $\widetilde{\mathfrak{A}}$ within the parameter space varies from rule to rule.

Regime boundaries also differ markedly as a function of the chosen entrainment rule. While the $\mathcal{I} = \mathcal{I}_{\text{crit}}$ boundary is mostly a function of D for solutions obtained with the CM rule, this boundary is more strongly dependent on SST for the NT and DL rules. The close relation between efficient entrainment and $\mathcal{I} > \mathcal{I}_{\text{crit}}$ is to be expected based on our previous analysis, wherein rules with $\widetilde{\mathfrak{A}}$ near unity generally entrain sufficient warm air to offset the radiative cooling completely, resulting in equilibria where heat must be additionally lost to the surface to balance the vigour of entrainment warming. In such cases we expect $\overline{w's'_{l0}}$ to be negative and $\mathcal{I} > 0$. In terms of CTEI, rules which entrain weakly enough to allow for buoyancy reversal tend to locate this regime at higher SSTs and greater values of D, indicating that this regime will be most likely for warmer and shallower layers. Although not shown, all models produce an $\mathcal{L} = 0.3$ kg m^{-2} contour which is relatively insensitive to SST and occurs at values of divergence which range from 3 to 5×10^{-6} s^{-1}.

Notwithstanding these differences, there are some broad classes of at least qualitatively similar behaviour. For instance, the NT and DL rules lead to patterns of $\widetilde{\mathfrak{A}}$ which are broadly similar, with the RK, AL and CM schemes behaving somewhat more uniquely. The broad similarity between the NT/DL rules is perhaps not unexpected, given their similar strategy for modelling the stability across the undulation layer and their neglect of a $\mathfrak{D}$ term. Their more pronounced sensitivity of $\widetilde{\mathfrak{A}}$ to SST is consistent with their incorporation of moisture fluxes ($\overline{w'q'_{t0}}$) in the energetics, their sensitivity to buoyancy reversal and hence $s_{l,+} - s_{l,s}$, and their lack of a $\mathfrak{D}$ term, which in the AL and CM rules introduce a strong dependence on $\mathcal{L}$ and hence D. The relatively greater dependence on q_l in the NT rule is also consistent with greater sensitivities to D at large values of D.

The RK rule is peculiar (incidentally showing behaviour similar to the historic rules, not shown) in that almost all of its equilibria are characterized by $\widetilde{\mathfrak{A}} > 1$ and equilibria states which violate the $\mathcal{I}$ criteria for a well mixed layer. The reason is that the very pronounced $\mathfrak{D}$ term, and the use of $\delta_m b$ rather than Δb to measure the stability across the undulation layer, requires entrainment to proceed very efficiently. This is particularly evident at larger values of SST and D where deepening the boundary layer regularizes $\mathfrak{A}$.

The differences among entrainment rules are crystallized by comparing results from the DL, AL and CM rules. All of these rules have been derived on the basis of LES, in the

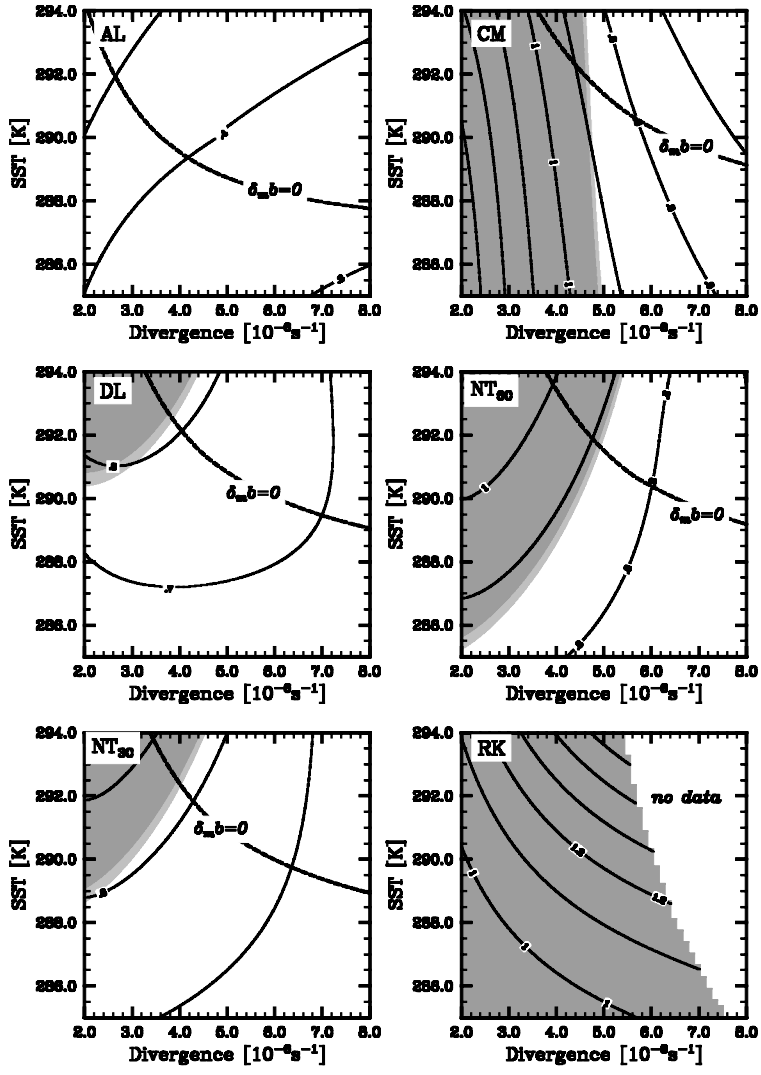

Figure 5. Level curves of $\widetilde{\mathfrak{A}}$ for steady states of the mixed-layer model closed with the entrainment rules described in section 3. Above and to the right of the buoyancy reversal boundary $\delta_{\mathrm{m}} b = 0$, the steady states have $\delta_{\mathrm{m}} b < 0$. Regions where $\mathcal{I} > 0.05$ are shaded in light grey, $\mathcal{I} > 0.1$ are shaded with darker grey. See text for further explanation.

case of CM and DL the same set of simulations were used to calibrate the entrainment rules. Nonetheless, values of $\widetilde{\mathfrak{A}}$ differ remarkably. The CM rule, which really does not incorporate moisture effects is relatively insensitive to SST. Instead, the tendency of the $\mathfrak{D}$ term to get larger as cloud depths (and hence $\mathcal{L}$) increase leads to increasingly larger values of $\mathfrak{A}$ as D decreases. The AL rule is, on the other hand, relatively insensitive to parameter values. Like the CM rule, it is strongly influenced by the $\mathfrak{D}$ term, but because $\mathfrak{D}_{\mathrm{AL}} \propto \exp(\mathcal{L})$ whereas $\mathfrak{D}_{\mathrm{CM}} \propto \exp(\sqrt{\mathcal{L}})$ this effect saturates more readily.

What might be the practical consequences of all this? We would expect that a large-scale model which used the AL scheme in its boundary-layer parametrization would more readily predict cloudy boundary layers, and perhaps predict them over a much larger area than the same large-scale model using one of the other rules. In addition we

might expect the climate sensitivity and cloud feedbacks of a climate model which used the CM rule in its boundary-layer parametrization to be substantially different to one which was based on a DL or NT class scheme. The latter would couple more tightly to processes which changed the SSTs while the former would couple more tightly to processes which changed D. Moreover if we take the $\mathfrak{I} > \mathfrak{I}_{\text{crit}}$ as a regime boundary for the STBL, then this suggests that relative to results based on other rules, models based on the RK schemes will tend to predict deeper layers which are less likely to be in the STBL regime.

(*c*) *Transients and adjustments*

Although the steady-state analysis is instructive and important to the basic dynamics of the system, it has long been understood that in some important respects actual mixed layers are probably far from equilibrium. Schubert *et al.* (1979b) pointed this out by showing that while the adjustment for the thermodynamic state of the boundary layer is of the order of a day, the boundary-layer depth adjusts on the time-scale of a week, which is much larger than an advective time-scale. Thus, memory is important to the system. We addressed these issues in three ways: (i) we looked at the Lagrangian trajectories of the mixed-layer models, similar to what was done by Schubert *et al.* (1979b), (ii) we looked at steady states of the model which included advective forcings, and (iii) we examined the transient behaviour of the solutions. As the transient behaviour becomes more important the differences among the rules tend to be reduced, however, the general pattern of results remains the same. Through a closer examination of the transient behaviour of the minimal model it is also straightforward to show that as far as the adjustment time-scale of the boundary-layer depth is concerned, the entrainment efficiency plays no role, but it does affect the adjustment time-scale for the thermodynamic variables—primarily indirectly by modifying the equilibrium boundary-layer height. In the case of s_l there is also a direct effect as the adjustment time-scale can be shown to depend explicitly on $\mathfrak{A}$.

5. Climatology

Before concluding we further explore how equilibrium solutions to the mixed-layer model might be useful in more directly exploring the climatology of marine stratocumulus. The approach we take here is quite similar to that used by Stevens (2002) to study the distribution of winds in the tropical Pacific. That is, we look at steady states of the model as a function of the climatological mean forcing. In the present case, such an approach has many shortcomings. Chief among these is the neglect of the long adjustment time-scales of the boundary-layer depth, and hence the cloud field. In addition, this approach neglects the effect of time variations in the forcing, and is susceptible to biases in the mean climatology. Despite these shortcomings the approach has value, and provides a basis for answering the question we are interested in, namely for plausible forcings what sort of range of steady states does the model predict? In particular we are interested in whether their geographic distribution is at all reasonable, and the extent to which this distribution is sensitive to the effective efficiency of the entrainment rule. In a sense our analysis repeats the analysis of the previous section, but it does so in a framework which is perhaps more relevant to the physical system.

For the forcing we use NCEP climatological June, July and August surface winds, surface divergence, 850 hPa temperatures and specific humidities, and the temperature gradients between 700 and 850 hPa, the latter being used to estimate the temperature

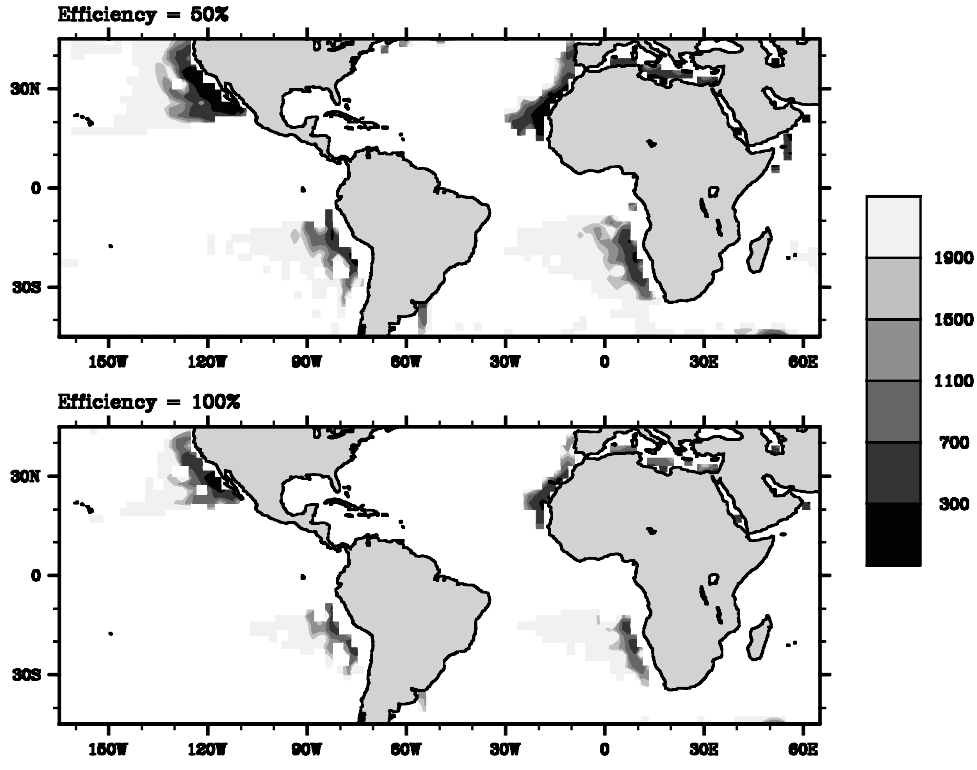

Figure 6. Boundary-layer depth h (m), for equilibrium solutions to the mixed-layer model, with an entrainment efficiency of $\mathfrak{A} = 0.5$ (top panel) and $\mathfrak{A} = 1.0$ (bottom panel), forced by climatological June–July–August forcings.

at levels other than at 850 hPa. Following the approach of previous sections we use a constant radiative forcing, in this case of 30 W m^{-2} (chosen to better approximate the diurnally averaged radiative forcing in the stratocumulus regimes), other fixed parameters take their values from Table 3. Results for the minimal model Eq. (50) for $\mathfrak{A} = 0.5$ and for $\mathfrak{A} = 1.0$ are given in Fig. 6.

Equilibrium solutions for both values of $\mathfrak{A}$ appear to represent well the major stratocumulus regions, and their structure. In both cases the boundary-layer depth is shallowest near the coast and increases as one moves offshore. In addition, the stratus regions tend to be most pronounced in the north-east trades as one would expect for this time of the year. Solutions for other seasons (not shown) also indicate that the response of the model is consistent with the seasonal cycle of stratocumulus over the world's oceans. In both cases the solutions are somewhat noisy, with regions of no solution surrounded by regions with physically realistic solutions. These variations can be tied directly to variations in surface divergence, which even in the climatological mean is relatively noisy, particularly in the south-east Pacific stratocumulus regions.

The effect of $\mathfrak{A}$ on the solutions is in accord with what we might expect based on the previous analysis. Solutions with smaller values of $\mathfrak{A}$ tend to have more pronounced stratus regions in shallower boundary layers. The small $\mathfrak{A}$ equilibrium solutions tend to have values of $\mathfrak{I}$ which are consistent with the maintenance of a mixed layer, while most of the $\mathfrak{A} = 1$ solutions tend to have values of $\mathfrak{I}$ more consistent with cumulus-coupled layers. In both cases the large $\mathfrak{I}$ solutions tend to be at the edge of the solution area.

This supports the climatological integrations of Bretherton and Wyant (1997) which indicated that regions where $\mathcal{I} > \mathcal{I}_{\text{crit}}$ effectively bound the climatological regions.

In some respects the small $\mathfrak{A}$ solutions *look* more realistic, but we caution against this interpretation. Because the adjustment time of the cloud layer can be long, actual boundary layers often reflect the climatological conditions well upstream (cf. section 4 and also Pincus *et al.* 1997). An analysis which we do not present here shows that the neglect of the adjustment process underestimates the extent of the STBL regime, so that it may well be that the $\mathfrak{A} = 0.5$ regime actually produces an STBL regime which is more extensive than observed. The point we wish to make here, is not which value of $\mathfrak{A}$ is reasonable, but rather if either seems plausible, and if both, to what extent the value of $\mathfrak{A}$ actually impacts on the solutions. Clearly both values of $\mathfrak{A}$ are plausible, but the differences are striking enough that a study which accounts for the adjustment process, time variability in the forcings, and possible biases in the climatology should be able to indicate which is more realistic, and the extent to which variations in $\mathfrak{A}$ along a trajectory (such as exhibited by the varied rules discussed in section 3) might have climatological significance. Such a study must account for the possible hysteresis in the solutions (Randall and Suarez 1984) and is currently under way.

6. Conclusions

At the outset we posed two questions: (1) how well do we really understand entrainment and (2) does it really matter? The answer to the first question is 'not very well'. The answer to the second question is 'yes'.

One of the primary objectives of this study was to attempt to synthesize recent studies of entrainment and evaluate their similarities and differences. In some ways the differences were remarkable. The AL and CM studies, both based on independent sets of large-eddy simulations, advocate entrainment efficiencies whose values differ by more than a factor of two. Even the CM and DL studies, which are based on the same set of simulations, are able to fit curves to those data which yield significantly different steady states. Other types of rules, based more on theoretical considerations and less on actual data (i.e. RK) tend to predict much larger entrainment velocities and equilibrium regimes which, by the mechanism of Bretherton and Wyant (1997) (expressed in terms of the criterion of Stevens (2000)), should be cumulus coupled over the entire parameter space.

In initiating this study it was understood that differing entrainment rates could substantially affect the short time evolution of large-eddy simulations of the STBL. What was unclear was the extent to which such differences might have climatological significance. For instance, just because parametrized entrainment rates differ substantially in one part of parameter space one should not automatically conclude that the equilibrium solutions will also differ substantially. Our study indicates that the range of entrainment rates exhibited by different rules would, in the absence of other feedbacks, have significant impacts on the climatology of a general-circulation model which was able to consistently implement their physics. Moreover, the sensitivities of the equilibria are sufficiently different that attempts to evaluate climate feedbacks due to changes in stratocumulus could depend on which entrainment rule is used.

While this is not a pleasing state of affairs the current situation is actually somewhat worse. Most general-circulation models do not consistently model the cloud-top interface in the marine stratocumulus regions, and as a result the entrainment rule they end up using is some complicated balance of numerical artefacts and physical processes, which is both difficult to evaluate and need not lie in the space spanned by existing

proposals. Thus, as far as improving parametrizations of stratocumulus in large-scale models is concerned, the first order of business is to properly represent the cloud-top interface. Given that the variability in $\widetilde{\mathfrak{A}}$ among rules is greater than the variability of $\widetilde{\mathfrak{A}}$ across parameter space for any given rule, even the consistent application of a very simple rule, such as Eq. (50) with $\mathfrak{A}$ constant, could constitute a great step forward.

From a more parochial perspective this work raises a number of other issues. One is that a study which attempts to evaluate the best entrainment rule based on climatology might be able to discriminate between more and less plausible entrainment rules. Another is that more work is necessary, based on simulations, to understand the differences in entrainment rates predicted by the LESs of various groups—work which would be more conclusive if it were based on steady-state solutions. The last is that observations of entrainment, specifically designed to test the predictions of the various models, are necessary. Work is currently under way on the first and last points. In terms of observations, data collected expressly for this purpose, in a series of flights in nocturnal stratocumulus off the coast of California in July 2001, are currently being analysed and will hopefully shed light on these questions. Combined with an evaluation of the climatology we are optimistic that estimates of entrainment efficiencies in stratocumulus can be greatly improved in coming years.

In closing we wish to emphasize a methodological point. As we stated at the outset, the mixed-layer model is the theoretical underpinning for our understanding of stratocumulus. With the advent of more sophisticated tools, such as large-eddy simulation, and increased accessibility to climate models, there is a tendency to leave behind, or forget, the simpler theoretical frameworks. This is a mistake. If anything, simple theories, such as the mixed-layer theory, are more relevant than they ever were. Both as a basis for interpreting and organizing results of large-eddy simulations or *in situ* observations, and as a basis for understanding the climatology of either large-scale models or the real atmosphere. Real advancements in our understanding of the interactions of stratocumulus and climate will be ephemeral if they are based only on simple comparisons of climate integrations, or calibrations of rules based on data and simulation. While such activities can contribute to our understanding, they can only do so when digested by a compellingly clear theoretical framework. For now, and the foreseeable future, this remains the mixed-layer theory of Lilly.

ACKNOWLEDGEMENTS

This work was supported by kind assistance from the National Science Foundation, Grant # ATM-9985413. The NCEP re-analysis data was provided by the National Oceanic and Atmospheric Administration Cooperative Institute for Research in the Environmental Sciences, Climate Diagnostics Center, Boulder, Colorado, USA, from their Web site at http://www.cdc.noaa.gov/. Comments by and discussions with Akio Arakawa, Celal Konor, Adrian Lock, Douglas Lilly, Chin-Hoh Moeng, Verica Savic-Jovcic and Margreet van Zanten greatly improved the manuscript.

APPENDIX

List of symbols

In Table A.1 we collect symbols whose meanings are not obvious and which are used repeatedly throughout the text. Many of these are heavily subscripted. The subscripts are used to specify where a variable locates and what variable or process it refers to. Subscripts pairs are: s and q which refer to liquid-water static energy, and

TABLE A.1. SELECTED SYMBOLS

Symbol	Denotes	Comment
$\mathfrak{A}$, $\mathfrak{W}$, $\mathfrak{D}$	Entrainment rule parameters	See Eq. (5), NB, $\widetilde{\mathfrak{A}}$ given by Eq. (49)
$\mathcal{B}$	Buoyancy flux	For $\mathcal{B}_{\Delta\mathcal{F}}$ see Eq. (14)
$\mathcal{F}$	Diabatic contribution to flux	$\mathcal{F}_{s,0}$, $\mathcal{F}_s$, $\mathcal{F}_{q,0}$, $\mathcal{F}_q$
$\mathcal{I}$	Buoyancy integral ratio	See Eq. (47)
$\mathcal{L}$	Liquid-water path	
β	Local efficiency	See Eqs. (7) and (8) also Eq. (18) for β_l
$\delta_\mathrm{d}b$, $\delta_\mathrm{m}b$	Buoyancy perturbations	See Eqs. (17) and (19) respectively
ϵ	Ratio of gas constants, $R_\mathrm{d}/R_\mathrm{v}$	Note that $\epsilon_1 \equiv 1/\epsilon - 1$
η	Global efficiency	See Eq. (11)
$\widehat{\eta}$	Modified efficiencies as per Lilly (2002)	See Eq. (42)
μ	Thermodynamic parameter	See Eq. (23)
$\widehat{\mu}$	Modified μ as per Lilly (2002)	
χ_*	Most saturated mixing fraction	See Eq. (20) and Fig. 3
ζ	(z_b/h) non-dimensional sub-cloud layer depth	
Δx	Jump of some variable x	E.g. $\Delta s_\mathrm{l} = s_\mathrm{l}(z_{i+}) - s_\mathrm{l}(z_{i-})$
ΔF	Radiative flux divergence	
Ψ	Buoyancy ratio	See Eq. (21)
b	Buoyancy	E.g. $\mathcal{B} \equiv \overline{w'b'}$
b_*	Buoyancy perturbation at χ_*	See Eq. (20) and Fig. (3)
h	Depth of mixed layer	Taken to equal z_{i-} in this analysis
q_t, q_v, q_*	Total, vapour and saturation specific humidities	Note that $q_\delta \equiv q_\mathrm{t} - q_*$
$q_\mathrm{l,max}$	Cloud-top liquid-water specific humidity	
s_l	Liquid-water static energy	$s_{l,0}$ denotes value at surface
z, z_{i+}, z_{i-}, z_b	Heights	See Fig. 1
C_D	Effective drag coefficient	
D	Divergence of horizontal winds	
E	Entrainment velocity	
G	Non-dimensional V	See Eq. (54)
H	Heaviside function	
T_v, T_0	Virtual and basic-state temperature	
$\|\mathbf{U}\|$	Average wind speed	
V	Radiative driving velocity scale	See Eq. (54)
W	Large-scale vertical velocity	Throughout $W \equiv -Dz$

total water respectively; h and 0 which refer to the boundary-layer top and surface respectively; m and d which refer to saturated (moist) and unsaturated (dry) processes respectively. So for instance $\mathcal{F}_{s,0}$ denotes the boundary flux of liquid-water static energy at the surface, while $\beta_{q,\mathrm{m}}$ denotes the efficiency with which moisture fluxes project onto buoyancy fluxes in saturated air. Exceptions to this pattern are the subscripts (l, t, b, * and v) which are used to denote liquid-water variables (static energy and specific humidity), total-water variables, cloud-base, saturation and virtual effects respectively

REFERENCES

Albrecht, B. A. 1991 Fractional cloudiness and cloud-top entrainment instability. *J. Atmos. Sci.*, **48,** 1519–1525

Bretherton, C. S. and Wyant, M. C. 1997 Moisture transport, lower tropospheric stability, and decoupling of cloud-topped boundary layers. *J. Atmos. Sci.*, **54,** 148–167

Bretherton, C. S., MacVean, M., Bechtold, P., Chlond, A., Cotton, W., Cuxart, J., Cuijpers, H., Khairoutdinov, M., Kosovic, B., Lewellen, D., Moeng, C.-H., Siebesma, P., Stevens, B., Stevens, D., Sykes I. and Wyant, M. 1999 An intercomparison of radiatively driven entrainment and turbulence in a smoke cloud, as simulated by different numerical models. *Q. J. R. Meteorol. Soc.*, **125,** 391–423

Deardorff, J. W. 1980 Cloud top entrainment instability. *J. Atmos. Sci.*, **37,** 131–147

Duynkerke, P. G. 1993 The stability of cloud top with regard to entrainment: Amendment of the theory of cloud-top entrainment instability. *J. Atmos. Sci.*, **50,** 495–502

Hartmann, D. L. and Short, D. A. 1980 On the use of Earth radiation budget statistics for studies of clouds and climate. *J. Atmos. Sci.*, **37,** 1233–1250

Klein, S. A. and Hartmann, D. L. 1993 The seasonal cycle of low stratiform clouds. *J. Climate*, **6,** 1587–1606

Konor, C. S. and Arakawa, A. 2001 'Incorporation of moist processes and a PBL parameterization into the generalized vertical coordinate model'. Technical Report 102, University of California Los Angeles, Department of Atmospheric Sciences, UCLA, Box 951565, Los Angeles CA 90095-1565, USA

Kraus, E. B. 1963 The diurnal precipitation change over the sea. *J. Atmos. Sci.*, **20,** 551–556

Kraus, H. and Schaller, E. 1978 A note on the closure in Lilly-type inversion models. *Tellus*, **30,** 284–288

Kuo, H.-C. and Schubert, W. 1988 Stability of cloud-topped boundary layers. *Q. J. R. Meteorol. Soc.*, **114,** 887–916

Lewellen, D. and Lewellen, W. 1998 Large-eddy boundary layer entrainment. *J. Atmos. Sci.*, **55,** 2645–2665

Lilly, D. K. 1968 Models of cloud-topped mixed layers under a strong inversion. *Q. J. R. Meteorol. Soc.*, **94,** 292–309

2002 Entrainment into cloud-topped mixed layers: A new closure. *J. Atmos. Sci.*, in press

Lock, A. 2000 The numerical representation of entrainment in parameterizations of boundary layer turbulent mixing. *Mon. Weather Rev.*, **129,** 1148–1163

1998 The parameterization of entrainment in cloudy boundary layers. *Q. J. R. Meteorol. Soc.*, **124,** 2729–2753

Ma, C.-C., Mechoso, C. R., Robertson, A. W. and Arakawa, A. 1996 Peruvian stratus clouds and the tropical Pacific circulation. *J. Climate*, **9,** 1635–1645

MacVean, M. K. and Mason, P. J. 1990 Cloud-top entrainment instability through small-scale mixing and its parameterization in numerical models. *J. Atmos. Sci.*, **47,** 1012–1030

Moeng, C.-H. 2000 Entrainment rate, cloud fraction and liquid water path of PBL stratocumulus clouds. *J. Atmos. Sci.*, **57,** 3627–3643

Moeng, C.-H. and Stevens, B. 1999 Marine stratocumulus and its representation in GCMs. Pp. 577–604 in *General circulation model development: Past, present, and future*. Ed. D. A. Randall. Academic Press

Moeng, C.-H., Bretherton, C., Cotton, W. R., Chlond, A., Khairoutdinov, M., Krueger, S., Lewellen, W., MacVean, M. K., Pasquier, J., Rand, H. A., Siebesma, A. P., Stevens, B. and Sykes, R. I. 1996 Simulation of a stratocumulus-topped PBL: Intercomparison among different numerical codes. *Bull. Am. Meteorol. Soc.*, **77,** 261–278

Moeng, C.-H., Sullivan, P. P. and Stevens, B. 1999 Including radiative effects in an entrainment-rate formula for buoyancy driven PBLs. *J. Atmos. Sci.*, **56,** 1031–1049

Neiburger, M., Johnson, D. S. and Chien, C.-W. 1961 'Studies of the structure of the atmosphere over the eastern Pacific ocean in summer'. Technical report, University of California, USA

Nicholls, S. and Leighton, J. 1986 An observational study of the structure of stratiform cloud sheets. Part I: Structure. *Q. J. R. Meteorol. Soc.*, **112,** 431–460

Paluch, I. R. and Lenschow, D. H. 1991 Stratiform cloud formation in the marine boundary layer. *J. Atmos. Sci.*, **48,** 2141–2157

Philander, S. G. H., Gu, D., Halpern, D., Lambert, G., Lau, N.-C., Li, T. and Pacanowski, R. 1996 Why the ITCZ is mostly north of the equator. *J. Climate*, **9,** 2958–2972

Pincus, R. and Baker, M. B. 1994 Effect of precipitation on the albedo susceptibility of marine boundary layer clouds. *Nature*, **372,** 250–252

Pincus, R., Baker, M. B. and Bretherton, C. S. 1997 What controls stratocumulus radiative properties? Lagrangian observations of cloud evolution. *J. Atmos. Sci.*, **54,** 2215–2236

Randall, D. A. 1980 Conditional instability of the first kind upside-down. *J. Atmos. Sci.*, **37,** 125–130

Randall, D. A. and Suarez, M. J.	1984	On the dynamics of stratocumulus formation and dissipation. *J. Atmos. Sci.*, **41,** 3052–3057
Randall, D. A., Abeles J. A. and Corsetti, T. G.	1985	Seasonal simulations of the planetary boundary layer and boundary-layer stratocumulus clouds with a general circulation model. *J. Atmos. Sci.*, **42,** 641–676
Schubert, W. H., Wakefield, J. S., Steiner, E. J. and Cox, S. K.	1979a	Marine stratocumulus convection. Part I: Governing equations and horizontally homogeneous solutions. *J. Atmos. Sci.*, **36,** 1286–1307
	1979b	Marine stratocumulus convection. Part II: Horizontally inhomogeneous solutions. *J. Atmos. Sci.*, **36,** 1308–1324
Shy, S. S. and Breidenthal, R.	1990	Laboratory experiments on the cloud-top entrainment instability. *J. Fluid Mech.*, **214,** 1–15
Slingo, J.	1980	Cloud parameterization scheme derived from GATE data for use with a numerical model. *Q. J. R. Meteorol. Soc.*, **106,** 747–770
Stevens, B.	2000	Cloud transitions and decoupling in shear-free stratocumulus-topped boundary layers. *Geophy. Res. Lett.*, **27,** 2557–2560
Stevens, B., Cotton, W. R., Feingold, G. and Moeng, C.-H.	1998	Large-eddy simulations of strongly precipitating, shallow, stratocumulus-topped boundary layers. *J. Atmos. Sci.*, **55,** 3616–3638
Stevens, B., Moeng, C.-H. and Sullivan, P. P.	1999	Large-eddy simulations of radiatively driven convection: Sensitivities to the representation of small scales. *J. Atmos. Sci.*, **56,** 3963–3984
Stevens, B., Duan, J., McWilliams, J. C., Münnich, M. and Neelin, J. D.	2002	Entrainment, Rayleigh friction and boundary layer winds over the tropical pacific. *J. Climate*, **15,** 30–44
Suarez, M., Arakawa, A. and Randall, D.	1983	The parameterization of the planetary boundary layer in the UCLA general circulation model: Formulation and results. *Mon. Weather Rev.*, **111,** 2224–2243
Turton, J. D. and Nicholls, S.	1987	A study of the diurnal variation of stratocumulus using a multiple mixed layer model. *Q. J. R. Meteorol. Soc.*, **113,** 969–1009
Twomey, S. A.	1974	Pollution and the planetary albedo. *Atmos. Environ.*, **8,** 1251–1256
	1977	The influence of pollution on the shortwave albedo of clouds. *J. Atmos. Sci.*, **34,** 1149–1152
Van Zanten, M. C., Duynkerke, P. G. and Cuijpers, J. W. M.	1999	Entrainment parameterization in convective boundary layers derived from large eddy simulations. *J. Atmos. Sci.*, **56,** 813–828
Von Ficker, H.	1936	Die Passatinversion. Pp. 1–33 in *Veröffentlichungen des Meteorologischen Institutes der Universität Berlin*